

**A speleothem precipitation record from Alabama spanning the last 12 thousand years:
links between Northern Hemisphere high-latitude cooling and Southeastern US
hydroclimate**

by

Stefan Perritano

A thesis Submitted to the Graduate Faculty of
Auburn University
in partial fulfillment of the requirements for the Degree of
Master of Science

Auburn, Alabama
May 2, 2020

Keywords: paleoclimate, geology, hydroclimate, teleconnections, stalagmite record

Approved by

Dr. Martín Medina-Elizalde, Chair, Associate Professor of Geology
Dr. Haibo Zou, Co-Chair, Professor of Geology
Dr. Matthew Waters, Assistant Professor of Environmental Sciences
Dr. Joe Lambert, Research Scientist (University of Alabama)

Table of Contents

1. List of Tables	2
2. List of Figures.....	3
3. Acknowledgments.....	4
4. Abstract	5
5. Introduction	6
6. Methods	9
7. Results and Discussion.....	21
8. Conclusion	38
9. References	40
10. Supplementary Figures	53

List of Tables

Table 1 (U-Th Data).....	17
Table 2 (Rainfall Data)	21
Table 3 (Calcite Equilibrium Equations).....	33

List of Figures

Figure 1.....	13
Figure 2.....	14
Figure 3.....	19
Figure 4.....	20
Figure 5.....	23
Figure 6.....	24
Figure 7.....	25
Figure 8.....	26
Figure 9.....	27
Figure 10.....	37

Acknowledgments

I want to express my deep gratitude to my adviser Dr. Martin Medina-Elizalde. His extreme enthusiasm for everything that he does is contagious and made me strive for excellence over the past two years. It was a joy to work under him and he has helped me grow as both a scientist and an individual in more ways than I can express. Dr. Matthew DeCesare was crucial to this research project. He spent countless hours in the lab running my samples and teaching me how to repel while taking time out of his personal schedule to conduct field work with me. It was an absolute blast and I am forever indebted to him for his constant support. I would also like to thank my thesis committee: Dr. Joe Lambert, Dr. Haibo Zou, and Dr. Matthew Waters, they were all extremely helpful and did not hesitate to help in any way they could. Without their combined knowledge and guidance, I would not have gone nearly as smoothly as it did. Dr. Bruce Railsback also took time out of his work schedule to teach me about thin section petrography and looked at my samples with me. This was extremely selfless, and I cannot thank him enough. I would also like to thank the owners of War Eagle Cave as it is privately, without them generously accommodating our needs the project would not have been started in the first place. Finally, I would like to thank my friends and family as they kept me in constant good spirits, and they were always there when things got tough. This thesis would not have been achievable without all those that I have mention and more, so thank you to everyone who has also helped in the past two years!

Abstract

I present a new stalagmite $\delta^{18}\text{O}$ record, named War Eagle 1, collected from War Eagle Cave in Northern Alabama that spans the interval between 12,222 years to 320 years before present (BP), thus offering a paleoclimate record of Holocene climate variability from the interior southeast United States (SEUS). I interpret this record to reflect an amount effect on interannual timescales and the relative contribution of summer relative to winter precipitation amount to the annual amount and isotopic budget. I find a close connection between hydroclimate variability in the SEUS, North Atlantic temperature variability and Caribbean hydroclimate. A consistent picture emerged whereby winter precipitation in the SEUS increases during events of high latitude cooling triggered by slowdown of North Atlantic deep-water formation, such as during the Younger Dryas and 8.2 ka cold events. In contrast, I find evidence suggesting that both summer and winter precipitation in the SEUS decrease across the transition from the 'Holocene Climate Optimum' to the 'Neoglacial', which is generally attributed to external orbital forcing.

Introduction

During the last 12 thousand years, Earth experienced a series of abrupt cold climate events superimposed onto a long-term cooling trend generally attributed to a decrease in northern hemisphere summer insolation. These cold events, referred to as the Younger Dryas, the 8.2 thousand-year ago (ka) event and the Little Ice Age have been hypothesized to originate in the northern hemisphere high-latitudes, around Greenland. The YD and 8.2 ka events, particularly, have been attributed to a slowdown of North Atlantic deep-water formation resulting in decrease ocean-atmospheric heat transport into the high latitudes. The extent to which these climate oscillations propagated beyond the North Atlantic high latitudes remains poorly known.

The Younger Dryas (12.8-11.8 ka) represents the major of these cold episodes. The prevailing hypothesis to explain the YD cold interval, proposed by (Broecker et al., 1989) suggested that an abrupt rerouting of Lake Agassiz overflow through the Great Lakes and St. Lawrence Valley inhibited deep water formation in the subpolar North Atlantic and weakened the strength of the Atlantic Meridional Overturning Circulation (AMOC). Global circulation model experiments and few available paleoclimate records suggest Gulf of Mexico, North Atlantic and Caribbean climate responded to the YD (Haug et al., 2001; Lea et al., 2003; Liu et al., 2012; Peterson and Haug, 2006). Gulf of Mexico (Oglesby et al., 1989; Schmidt and Lynch-Stieglitz, 2011) and Caribbean SSTs (Lea et al., 2003) were significantly colder than today. As suggested by sediment Ti and Fe percent records from the Cariaco Basin (CB), Venezuela, the mean position of the ITCZ in the summer was displaced southward from its current position (Haug et al., 2001; Peterson and Haug, 2006). This pattern of colder North Atlantic SSTs, a southern displacement of the ITCZ and drought in the Caribbean and northern South America is a consistent pattern also observed during the Little Ice Age time interval (Haug et al., 2001;

Peterson and Haug, 2006), and a robust feature of hosing experiments with global circulation models (Dahl et al., 2005; Lohmann and Lorenz, 2000; Otto-Bliesner and Brady, 2010; Stouffer et al., 2006; Vellinga and Wood, 2002). Low latitude northern hemisphere declines in precipitation during AMOC shutdown is supported by paleoclimate records from the last glacial interval as well (Deplazes et al., 2013; Medina-Elizalde et al., 2017).

The 8.2 Ka BP event was first identified within the Greenland ice core records as the most distinctive isotopic excursion of the Holocene. The event is typified as a rapid temperature decrease at Summit Greenland down by 7°C relative to the preceding time (Johnsen et al., 1997; Dansgaard, 1993; Alley et al., 1997) and lasting roughly 160 years during which decadal-mean isotopic values were below average. Within this event a central event of ~69 years has been identified with isotopic values consistently more than one standard deviation below the average relative to the preceding period (Thomas et al., 2007). The proposed mechanism for the 8.2 ka event is similar to the YD. The 8.2 ka event is also attributed to a decrease in the ocean heat transfer to the atmosphere driven by a slowdown of North Atlantic Deep water formation (Barber et al., 1999; Clark, 2001). As the Laurentide ice sheet melted in the early Holocene, large amounts of freshwater were stored in the lakes of Agassiz and Ojibway in North America. Once the Hudson Bay Ice Saddle collapsed the freshwater input, from both the draining of the proglacial lakes and melting of the Hudson Bay Ice Saddle, entered the Hudson Bay and in extension the North Atlantic; causing a large-scale density restructuring event, which slowed deep water formation and the thermohaline circulation (Ellison et al., 2006). Freshening of the North Atlantic is supported by paleoclimate evidence (Jakobsson et al., 2001) and the observed atmospheric and ocean responses are also supported by climate model experiments (LeGrande et al., 2006; Renssen et al., 2002). There is evidence from Europe that suggest that this event spread

beyond Greenland, but the signal beyond the North Atlantic becomes weaker (Alley and Agustsdottir, 2005; Rohling and Palike, 2005). Examination of proxy record from around the globe suggest that although anomalies in climate proxy records are often correlated with this sharp event in Greenland, anomalies in many of these records span 400 to 600 years, thus are much longer than the event in Greenland (Rohling and Palike, 2005). It is suggested that only anomalies in proxy record which are coeval with the 8.2 ka event in Greenland to be coined such event (Rohling and Palike, 2005; Thomas et al., 2007).

Climatic drivers in the interior Southeastern United States (SEUS) are poorly constrained and have been a topic of debate (Wanner et al., 2008). Climate models for the interior SEUS disagree with each other, predicting precipitation changes ranging from -30% to +35% and temperature changes from -2°C to +6°C by the year 2099 (Anandhi and Bentley, 2018). This significant variation in future climate predictions highlights the need to better understand regional climate and its potential drivers, particularly on decadal and longer timescales.

Teleconnections between high-latitude climate variability and hydroclimate variability in the SEUS over the Holocene remain poorly understood. There are currently very few paleoclimate records from the SEUS that cover at least partially the last 12 kyr and none span the YD and 8.2 ka events (Pollock et al., 2016; Stahle and Cleveland, 2002; Driese et al., 2016; Aharon and Dhungana, 2017). This lack of continuous paleoclimate records mainly reflects the absence of suitable archives for climate reconstruction, including the current lack of old growth trees, natural lakes, and glaciers within this region.

Stalagmite oxygen isotope ($\delta^{18}\text{O}$) records offer a unique opportunity to reconstruct the long-term history of precipitation variability and extreme events from interannual to orbital timescales (Aharon and Dhungana, 2017; Done et al., 2009; Frappier, 2009; Medina-Elizalde et

al., 2010; Medina-Elizalde et al., 2016; Walsh et al., 2016). Currently, there are only two stalagmite high-resolution climate records available from the SEUS, one from Alabama, spanning from 6 to ~1 ka (Aharon and Dhungana, 2017) and another from West-Central Florida, spanning 6.6 – 4.6 ka (Pollock et al., 2016). These records have high resolution and have revealed novel information about the role of decadal and multidecadal hydroclimate variability in the SEUS.

Here we present a hydroclimate record based on stalagmite $\delta^{18}\text{O}$ and $\delta^{13}\text{C}$ from the southeastern United States, spanning the last ~12 ka and the crucial YD cold interval, 8.2 ka event and Little Ice Age. Thus, the new record allows us to examine subtropical climate responses within the SEUS to high-latitude climate forced by shifts in the thermohaline circulation. There is an interest in determining the actual geographical extent of the YD, 8.2 ka and LIA events beyond the circum-North Atlantic region, especially if climate proxy records representing these events are to be used in helping validate models of thermohaline circulation shifts, in the context of potential changes in deep water formation during the Anthropocene.

Methods

a. Study Area

In 2017, we retrieved a stalagmite specimen, named War Eagle (WE), from an isolated cave chamber within War Eagle (WE) Cave in Marshall County, Alabama (Figure 1). The cave is located on private property and is accessible for only half of the year, because of hunting season. War Eagle Cave possesses one entrance, a collapsed skydome requiring a 41m repel, and is hosted within the Bangor Limestone. The thickness of the epikarst where the stalagmite was found is estimated to be between 30 and 35 m. The soil on the cave's exterior surface is extremely scarce. The USDA categorized the surface as stony colluvial, rockland limestone, and

rockland sandstone (USDA). Bangor limestone is a medium gray bioclastic, and oolitic limestone (Szabo et al., 1988). WE-1 had previously been broken from its base and was found lying on one side. WE-1 is 344 mm in length and has distinctive laminations, which do not represent annual depositions as suggested by U-Th dating (more details below).

b. Local and regional climatology

Long-term instrumental climate records (1981-2010) from NOAA's weather station in Scottsboro, AL (34.6736N, 86.0536W) indicate mean annual precipitation in the locality of WE Cave is 1,446 mm, and mean annual temperature 15.5°C. Precipitation is moderately variable and shows little seasonality, with the lowest monthly rainfall amount typically observed in October (87.3 mm) and the highest in December (145.2 mm) (Figure 2). Monthly temperature variations range from the lowest in January (4.3°C) to highest in July (26°C) (ncdc.noaa.gov). Alabama, like many other locations in the interior southeast, has nearly the same amount of precipitation in the warm season as in the cool season. Regional winter precipitation amount can slightly dominate the annual budget (29%), followed by spring and summer (~25% each) and lastly, fall season (~20%) (data from Tuscaloosa, Alabama, 2005-2015) (Dhungana and Aharon, 2019; Lambert and Aharon, 2010).

Spatial correlation analyses of the instrumental record of precipitation across the SEUS, Caribbean and Gulf of Mexico region relative to the precipitation record from Birmingham Alabama, suggest that the SEUS experiences the same climatological regime on interannual time scales. Relative to the Gulf of Mexico and Caribbean regions, the precipitation variability in the SEUS is anticorrelated with that from that in those regions (Figure 1). The latter is a result of most of the SEUS experiencing almost no seasonality regarding precipitation, as mentioned above, whereas the Gulf of Mexico and Caribbean regions, having marked seasonality, with peak

precipitation during the “Rainy” season, from June to October, and precipitation minima during the “Nortes” and “Dry” Seasons, from November to May ((Karmalkar et al., 2011; Magaña et al., 1999).

The spatial and temporal pattern of summer precipitation in the SEUS is influenced by convective systems (Baigorria et al., 2007), synoptic-scale systems such as tropical cyclones (Barlow, 2011; Konrad, 1997; Konrad II and Perry, 2010), and large-scale circulation changes (Li et al., 2013). Studies suggest that both Pacific and Atlantic SSTs influence SEUS summer precipitation. For example, El Niño Southern Oscillation (ENSO) has been suggested to influence SEUS precipitation with seasonally dependent impacts (Enfield, 1996; Mo and Schemm, 2008). North Atlantic SSTs have also been found to play an important role in summertime regional precipitation whereby North Atlantic warming on interannual timescales decreases precipitation over the SEUS (Enfield, 1996; Wang et al., 2008; Wang et al., 2010). North Atlantic SSTs, associated with the Atlantic Multidecadal Oscillation (AMO), impact regional summer precipitation via tropical cyclone activity and shifts in the southerly Great Plains low level jet (Curtis, 2008; Wang et al., 2010). The subtropical North Atlantic ocean, the Mexican Caribbean and the Gulf of Mexico regions represent the main source of year-round moisture for precipitation in large areas of the continental US and particularly the SEUS (Drumond et al., 2011; Gimeno et al., 2012). During the spring and winter seasons, mid-latitude cyclones advect moisture from the Gulf of Mexico and North Atlantic into the SEUS (Keim, 1996). The SEUS also experiences a characteristic increase in precipitation recycling with precipitation of terrestrial origin during the summer (Dominguez et al., 2006). Oceanic sources of moisture, however, are dominant, and recycling only becomes important during drier periods when the amount of external moisture is reduced (Gimeno et al., 2012). Li et al., (2013),

examining multiple reanalysis datasets, find that the North Atlantic Subtropical High western ridge position is a primary regulator of interannual variation of moisture transport to the SEUS and that dynamical processes (atmospheric circulation) represent the main source of moisture.

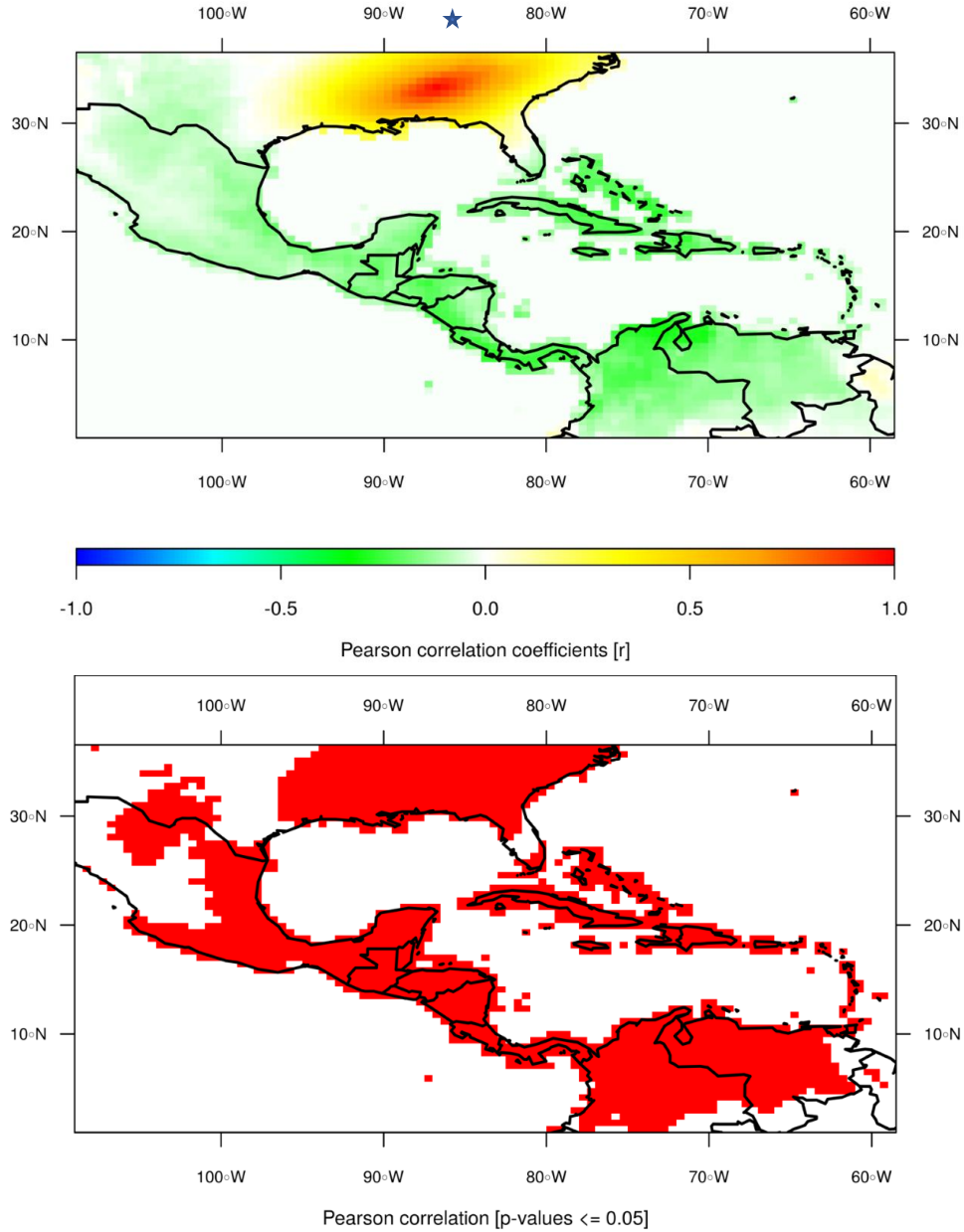


Figure 1: Spatio-temporal correlation analysis of precipitation (monthly values from 1901 to 2013 and with a spatial coverage of 0.5° latitude by 0.5° longitude) at the location ($34^\circ 31'N$, $86^\circ 11'W$) (War Eagle Cave, Alabama). Location of War Eagle Cave indicated with light blue star. The precipitation data set comes from the GPCC Global Precipitation Climatology Centre.

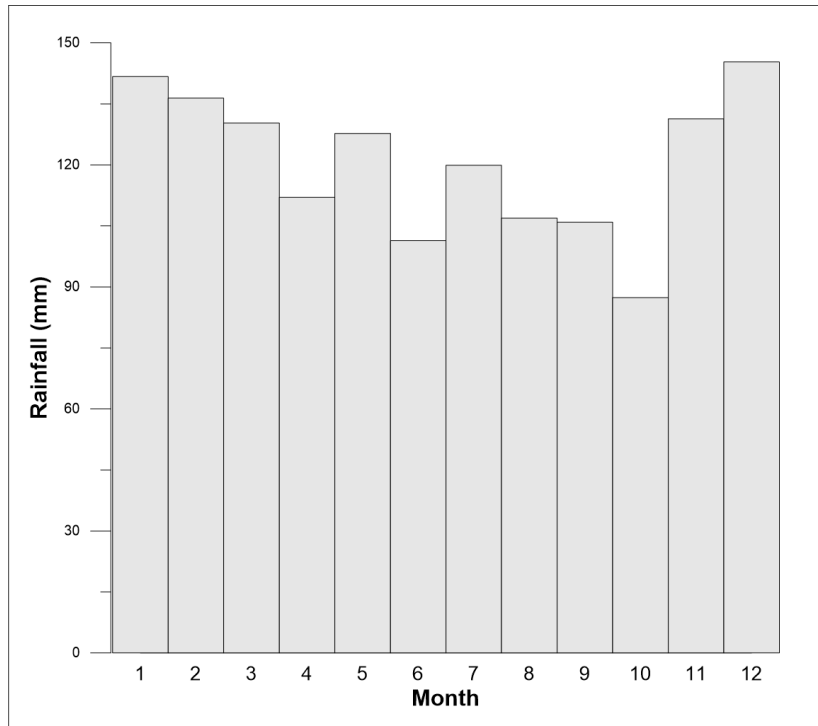


Figure 2. Graph of monthly rainfall for the period 1981-2010 for Scottsboro, Alabama Months 1-12, Jan-Dec, respectively (www.ncdc.noaa.gov).

c. Cave Monitoring

War Eagle cave monitoring was established in order to better understand cave environmental conditions, particularly temperature and relative humidity, both factors affecting the isotopic fractionation between drip water and stalagmite calcite. Two ONSET-HOBO instruments were placed inside of the chamber where WE specimen was found, from October 2018 to October 2019. These instruments were replaced in March 2019 in order to avoid saturation of the humidity sensors. Monitoring results indicate WE Cave remained at or near saturation conditions (RH 100%) and thermally stable year-round with a constant temperature of 14.7°C, thus very close to the mean surface atmospheric temperature in the area, providing evidence that WE cave have conditions conducive to minimizing kinetic effects, favoring isotopic equilibrium between calcite and drip water. Moreover, the thermal stability of the cave,

with temperature resembling mean annual air surface temperature, suggest that it is in thermal equilibrium and probably responds only to long-term surface temperature changes, similar to what is observed in other cave systems, in the tropics (Lases-Hernandez et al., GCA 2019) (Supplementary Figure 1). In addition, we placed a water drip collector, following the protocol by Lases-Hernandez et al., GCA 2019, and collected water uninterruptedly from a drip site over the course of one year. Because of the difficult and dangerous access to War Eagle cave, we were only able to collect two 6-month water samples (PC1= September 2018-March 2019 and PC2=April 2019-September-2019). The same isotopic result from these two temporally different samples ($\delta^{18}\text{O} = -5.9 \text{ ‰}$), similar to values of the amount weighted $\delta^{18}\text{O}$ composition of rainfall typically observed in Tuscaloosa, suggest drip water integrates several months and perhaps few years of precipitation amount. We note that this study is not concerned with seasonal and even year-to-year rainfall variability because WE stalagmite $\delta^{18}\text{O}$ samples integrate between 7 and 44 years of calcite growth.

d. Chronology

The WE-1 speleothem time scale was determined by 17 absolute U/Th dates (Table 1), following the methods by Cheng et al. (2013) and Shen et al. (2003, 2012). Calcite powders weighing 50 to 130 mg were used for Uranium and Thorium chemistry (Shen et al., 2003). U-Th isotopic measurements were conducted on a multi-collector inductively coupled plasma mass spectrometer (MC-ICP-MS), Thermo Fisher Neptune, at the David McGee Laboratory in the Massachusetts Institute of Technology (Shen et al., 2012). A triple-spike, ^{229}Th - ^{233}U - ^{236}U , isotope dilution method was employed to correct for mass bias and determine all uranium and thorium isotopic and concentration values in an off-line data reduction process developed by Shen et al. (2003). All errors of isotopic data and dates given are two standard deviations. Age

uncertainties ranged from ± 15 to ± 110 years with a mean of ± 40 years. Only one date has an uncertainty of ± 110 years and the remaining 16 dates have uncertainties lower than ± 70 years, across the 12-thousand-year record.

U-Th dates indicate that WE stalagmite grew over three-time intervals separated by two hiatuses. Briefly, WE began to grow 12.2 thousand years (kyr) before present (BP) and stopped growing 10.8 kyr BP. After an interruption of over 1 kyr, the stalagmite resumed growth 9.4 kyr BP and stopped growing 4.3 kyr BP. Finally, after a ~ 2 kyr interruption, the stalagmite resumed growth once again 2.6 kyr BP and stopped growing 300 years BP (years BP are relative to C.E. 1950). These two hiatuses are visually distinctive as a shift in color, fabric and vertical growth orientation (Supplementary materials Figure 2). Importantly, the stalagmite spans the time intervals of interest corresponding to the Younger Dryas, 8.2 kyr event and the Little Ice Age of northern hemisphere high latitude climate variability. We developed the chronology of these sections based on a piecewise-linear model to account for apparent slight non-linearity in stalagmite growth (Supplementary materials Figure 3).

Table 1 U-Th dates for speleothem War Eagle-1

Sample ID	Distance (mm)	²³⁸ U (ng/g) ^a	²³² Th (pg/g) ^a	δ ²³⁴ U (per mil) ^b	δ ²³⁴ U initial (per mil) ^c	Age (yr BP) (corrected) ^f	± (2σ)
WE-13	1.64	5870	5820	397	± 398	314	± 13
WE-5	14.96	5150	5810	387	± 389	1277	± 15
WE-16	20	4740	6060	380	± 383	2360	± 30
WE-17	27.4	7310	1510	375	± 378	2670	± 20
WE-14	33	5640	2750	324	± 328	4300	± 30
WE-6	54.82	8480	8440	290	± 294	5090	± 20
WE-15	73.5	11200	1090	298	± 303	5290	± 30
WE-7	87.56	5220	6560	312	± 317	5810	± 30
WE-4	103.8	7810	2380	350.3	± 357	6874	± 20
WE-8	133.15	10300	3640	404	± 414	8000	± 40
WE-9	189.68	7070	8400	404	± 414	8450	± 40
WE-10	237.72	10000	6700	405	± 416	9340	± 40
WE-3	245.13	9140	21300	396.3	± 407	9414	± 57
WE-2	249.32	5890	54400	404.4	± 417	10810	± 110
WE-11	263.8	6470	15400	416	± 430	11030	± 60
WE-12	298.9	10600	49000	442	± 457	11560	± 70
WE-1	334.54	10300	8310	415.5	± 430	12089	± 51

Analytical errors are 2s of the mean.

$$^a d^{234}\text{U} = ([^{234}\text{U}/^{238}\text{U}]_{\text{activity}} - 1) \times 1000.$$

^b $d^{234}\text{U}_{\text{initial corrected}}$ was calculated based on ²³⁰Th age (T), i.e., $d^{234}\text{U}_{\text{initial}} = d^{234}\text{U}_{\text{measured}} \times e^{1234 \times T}$, and T is corrected age.

$$^c [^{230}\text{Th}/^{238}\text{U}]_{\text{activity}} = 1 - e^{-1230T} + (d^{234}\text{U}_{\text{measured}}/1000)[I_{230}/(I_{230} - I_{234})](1 - e^{-(1230 - 1234)T}), \text{ where } T \text{ is the age.}$$

Decay constants are $9.1577 \times 10^{-6} \text{ yr}^{-1}$ for ²³⁰Th, $2.8263 \times 10^{-6} \text{ yr}^{-1}$ for ²³⁴U (Cheng et al., 2000), and $1.55125 \times 10^{-10} \text{ yr}^{-1}$ for ²³⁸U (J

^d Age (relative to chemistry date of July 2012) corrections were calculated using an ²³⁰Th/²³²Th atomic ratio of 4 (± 2) ppm.

Those are the values for a material at secular equilibrium, with the crustal ²³²Th/²³⁸U value of 3.8. The errors are arbitrarily assumed

^e $d^{234}\text{U}_{\text{initial corrected}}$ was calculated based on ²³⁰Th age (T), i.e., $d^{234}\text{U}_{\text{initial}} = d^{234}\text{U}_{\text{measured}} \times e^{1234 \times T}$, and T is corrected age.

e. δ¹⁸O & δ¹³C Time Series'

The oxygen (δ¹⁸O) and carbon (δ¹³C) data was obtained at the Paleoclimate and Stable Isotope Laboratory in the Department of Geosciences at Auburn University, Alabama. Along the main growth axis 688 calcite powder micro samples were drilled at a sampling resolution of 0.5 mm. The carbon and oxygen isotopic composition of calcite powders were analyzed with a Thermo Scientific Delta V Plus Isotope Ratio Mass Spectrometer interfaced with a Thermo Gasbench II. The corresponding calcite oxygen isotope ratios are recorded in delta notation ‰ (δ¹⁸O). Long-term (3 year) reproducibility for reference standard IAEA-603 is

0.09‰ and 0.07‰ for $\delta^{18}\text{O}$ and $\delta^{13}\text{C}$ respectively. Reproducibility of $\delta^{18}\text{O}$ and $\delta^{13}\text{C}$ (average standard deviation for each sample of the War Eagle dataset) were 0.06‰ and 0.06‰, respectively.

f. Amount Effect

In this study we examined a 10-year record (2005-2015) of precipitation amount and $\delta^{18}\text{O}$ data produced by the University of Alabama (Dhungana and Aharon, 2019; Lambert and Aharon, 2010) provided by Dr. Rajesh Dhungana, in order to investigate the existence of an amount effect on seasonal and interannual time scales (Fig. 3 and 4). This important dataset allows us to investigate how different seasons contribute to interannual changes in precipitation amount and precipitation $\delta^{18}\text{O}$. In addition, we established a rain gauge on the top of the Haley Center Building at Auburn University to collect six months of rainfall data from October 2018 to March 2019. During this sampling interval we captured the isotopic signal of Hurricane Michael, which was the third most intense hurricane to make landfall in the contiguous United States. The rainfall $\delta^{18}\text{O}$ signal of this tropical cyclone event far exceeded all the isotopic values observed in the instrumental record with an isotopic composition of -11.2‰ (Table 2).

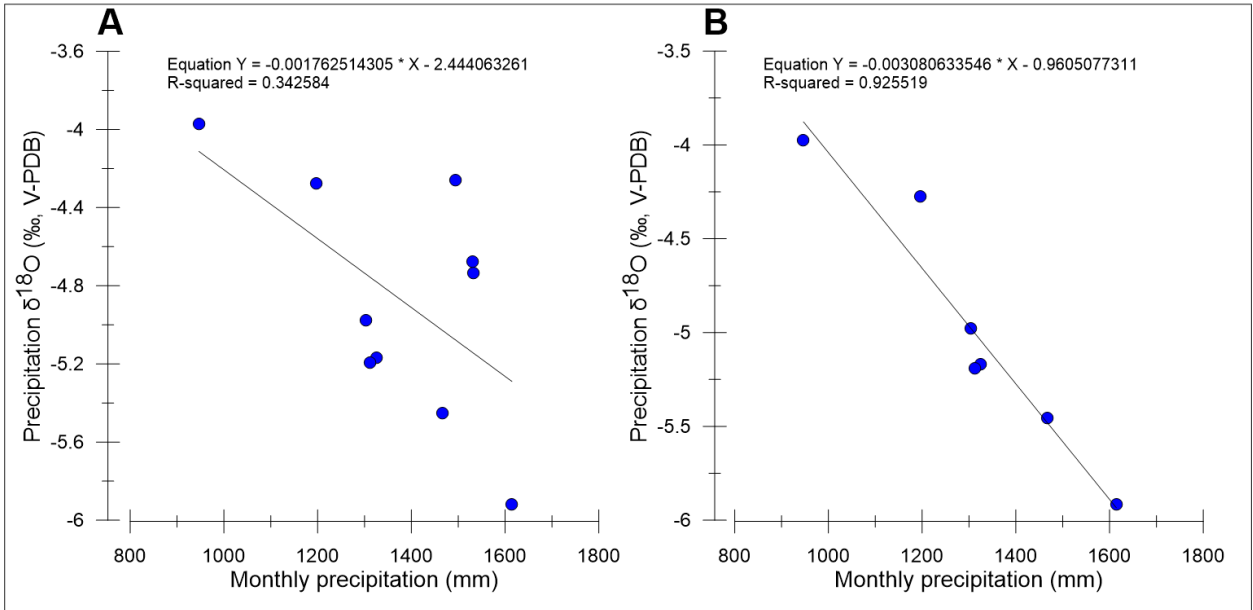


Figure 3: Precipitation amount and d18O composition from Tuscaloosa Alabama, spanning the time interval between 2005 and 2015 (Dhungana and Aharon, 2019; Lambert and Aharon, 2010). All the data combined (A) suggests a modest amount effect on interannual timescales. Removal of three outlier years (B) suggests a stronger amount effect on interannual timescales.

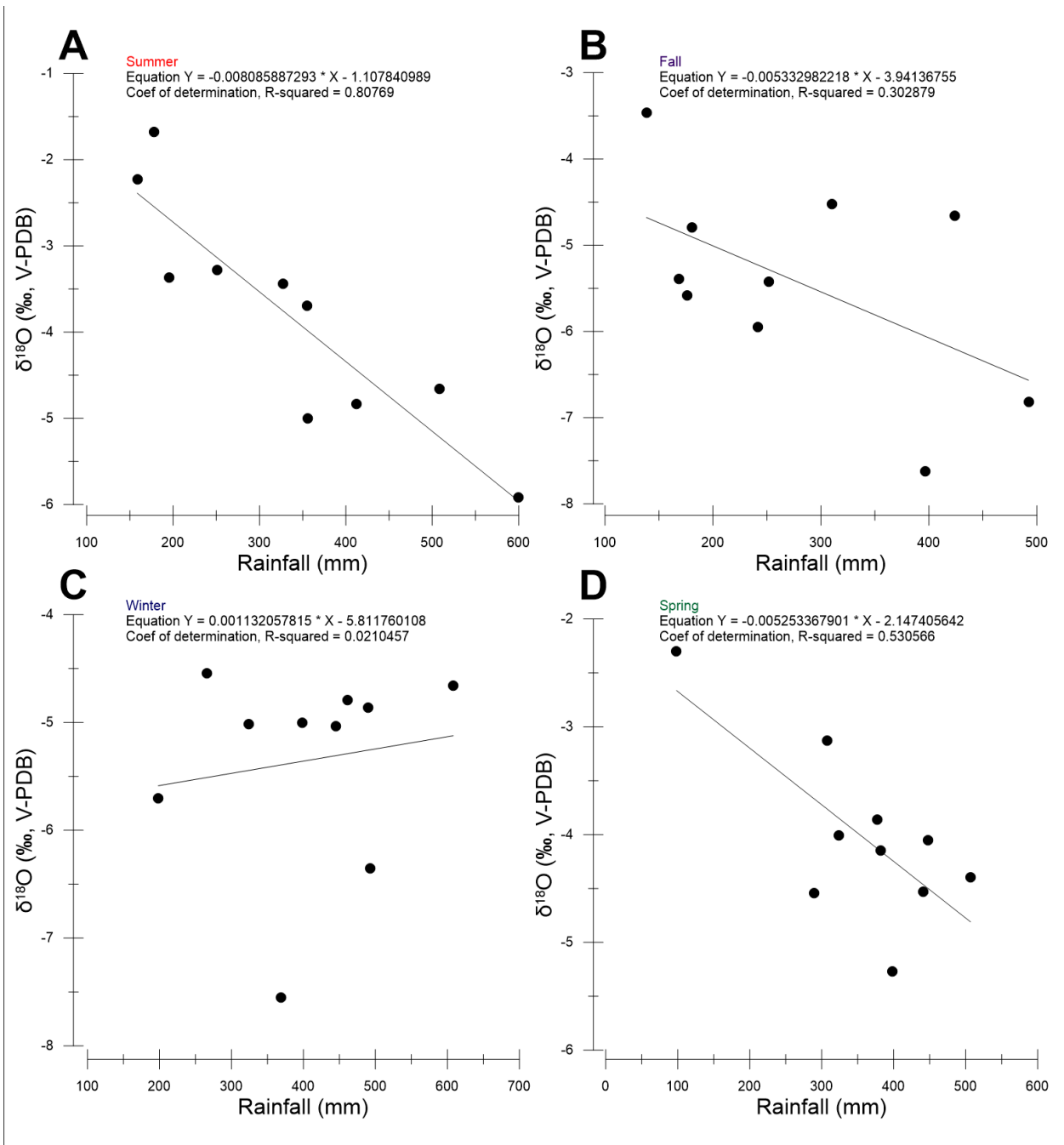


Figure 4: Analysis of the relationship between precipitation amount and precipitation $\delta^{18}O$ (amount effect) of season observed interannually, based instrumental data collected at the University of Alabama, from year 2005 to 2015 (Dhungana and Aharon, 2019; Lambert and Aharon, 2010). A distinctive amount effect is observed during the summer season interannually (A) a weaker amount effect during the fall (B) and spring seasons (D) and no effect during the Winter (C).

Table 2: Rainfall amount and $\delta^{18}\text{O}$ data that was collected from on top of the Haley Building in Auburn, Alabama. Collection occurred from 9/27/18 to 5/22/19.

Sample #	Date Collected	D18O	Precipitation (mL)	Notes
1	9/27/18 to 10/9/18	-6.64	990	
2	10/9/18 to 10/16/18	-11	2600	HURRICANE MICHAEL
3	10/16/18 to 11/15/18	-6.18	3550	
4	11/15/18 to 1/25/19	-5	7700	
5	1/26/19 to 2/27/19	-3	5070	
6	2/27/19 to 4/16/19	-5	8695	
7	4/17/19 to 5/22/19	-6	8480	

Results and Discussion

a. WE stalagmite $\delta^{18}\text{O}$ variability

We focus results and discussion sections on the WE stalagmite $\delta^{18}\text{O}$ record, although we also examine the $\delta^{13}\text{C}$ series on crucial time intervals. The WE stalagmite isotope records span the interval between 12.2 kyr BP and 0.3 kyr BP with two long hiatuses. We note that thin sections over these two hiatuses indicate they were associated with dry conditions (Supplementary Figure 4 and 5). WE stalagmite long-term average $\delta^{18}\text{O}$ composition is -3.3 ‰, with a range from -4.3‰ to -2.1 ‰ (Figure 5). Mean temporal resolution of the stalagmite record ranges between 7 and 44 years, with the highest mean resolution and growth rates occurring during the earliest part of the record and decreasing progressively towards the present. We examine the stalagmite $\delta^{18}\text{O}$ and $\delta^{13}\text{C}$ records in three separate sections, interrupted by the two hiatuses discussed previously, and label these sections based on the time interval they represent as, Early Holocene (EH), Middle Holocene (MH) and Late Holocene (LH).

The EH stalagmite $\delta^{18}\text{O}$ section is characterized by a multi-centennial cycle beginning 12.2 kyr BP and ending 10.8 kyr BP with positive $\delta^{18}\text{O}$ compositions of -2.8 ‰. The cycle peaks at 11.5 kyr BP with the most negative $\delta^{18}\text{O}$ values of this section \sim -4 ‰ (Figures 5 and 6).

Notably, the stalagmite ceases to grow when $\delta^{18}\text{O}$ plunges to the most positive values in the section (-2.5‰) and the full cycle closely corresponds to northern hemisphere high-latitude variability associated with the Younger Dryas time interval (more details below). Regarding the MH section, the stalagmite $\delta^{18}\text{O}$ record shows no discernable long-term trend between 9.4 and 7.8 kyr BP, although we note a significant negative $\delta^{18}\text{O}$ excursion centered at ~ 8.2 kyr BP (Figs. 5 and 7). Between 7.8 and 6 kyr BP, the stalagmite isotopic record shows a positive long-term trend associated with an isotopic shift of $\sim +1.2\text{‰}$. Following this trend, the stalagmite $\delta^{18}\text{O}$ record shows two prominent isotopic cycles between 5.5 kyr BP and 4.3 kyr BP. These cycles have an isotopic amplitude of 1.5-2 ‰ (Figs. 5 and 8). Concerning the LH section, the WE $\delta^{18}\text{O}$ record does not show a trend between ~ 2.6 and 1.5 kyr BP. After this time, the record shows a negative isotopic trend which peaks between 1 and 0.3 kyr BP, with isotopic values ranging between -3.2 and -3.7‰ . The $\delta^{13}\text{C}$ record generally follows the same pattern as $\delta^{18}\text{O}$ during almost the entire duration of these records. There is a notable divergence between the two isotopic records between 2 and 1.3 kyr BP, when they are out of phase (Figure 5 and 9).

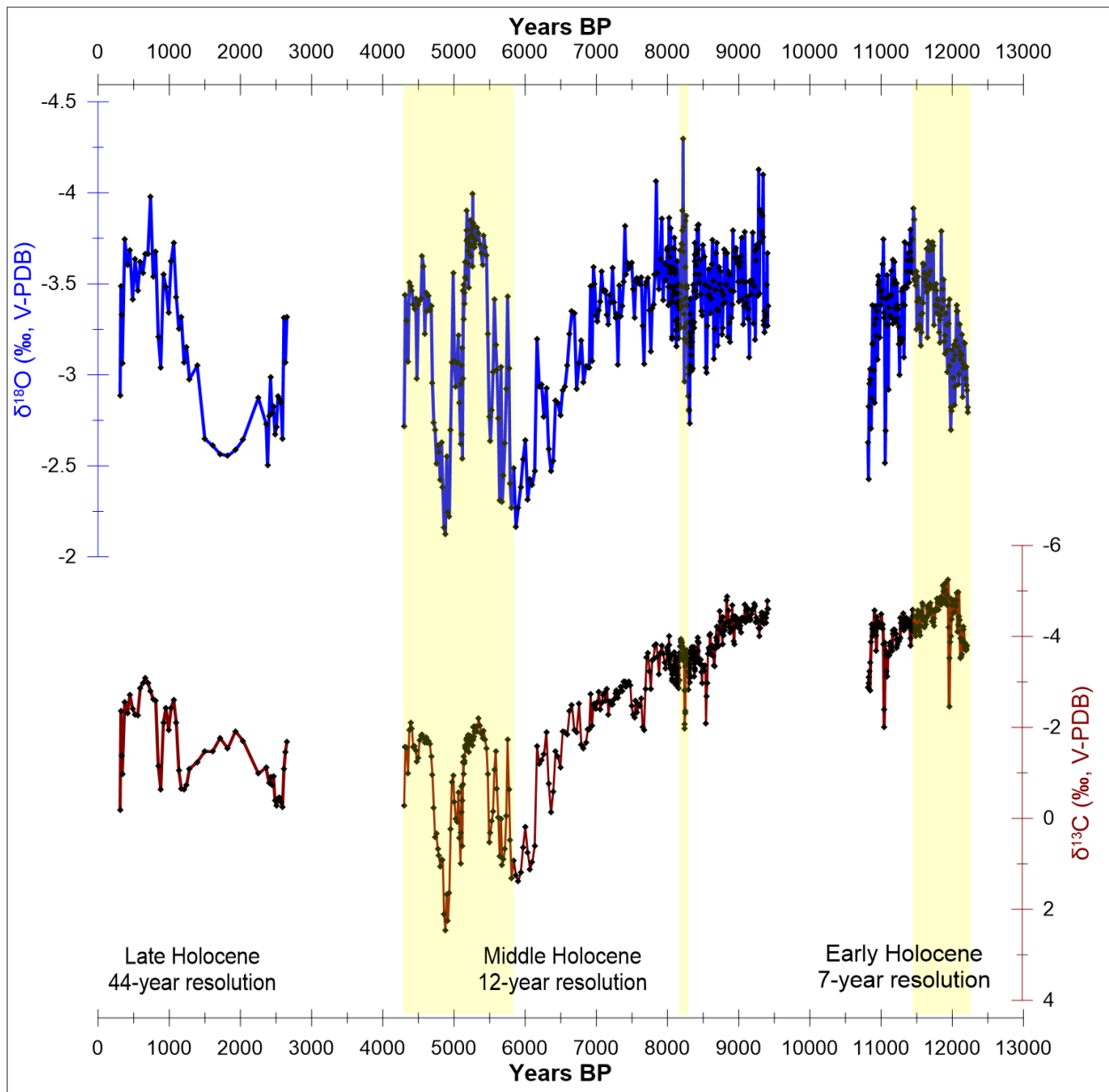


Figure 5: War Eagle-1 stalagmite $\delta^{18}\text{O}$ and $\delta^{13}\text{C}$ record. Yellow bars represent the YD, 8.2 kya event, and a period of increased variability.

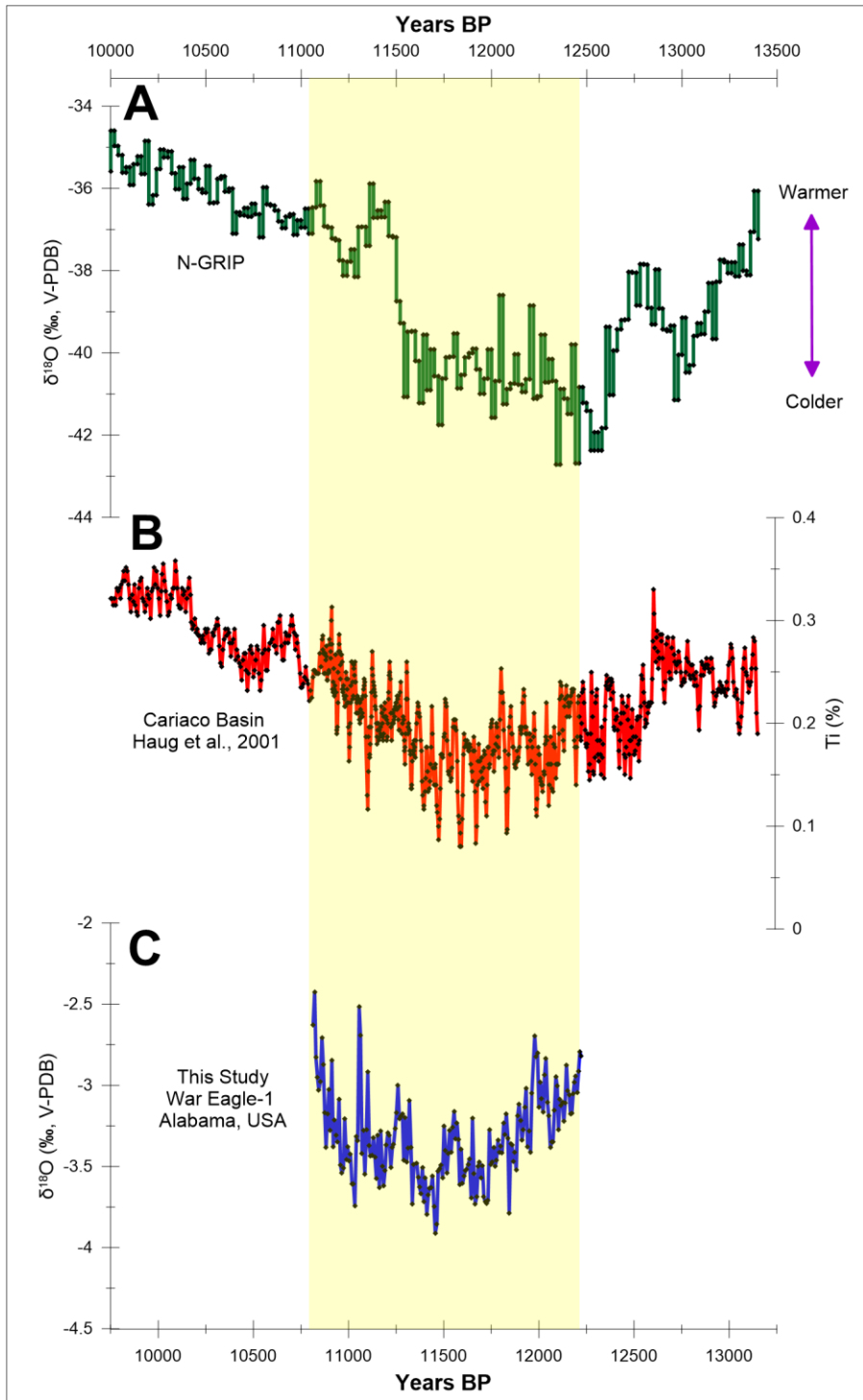


Figure 6: Comparison between WE-1 early Holocene $\delta^{18}\text{O}$ (C), Cariaco Basin Ti% record (B), and N-GRIP $\delta^{18}\text{O}$ record (A). The yellow bar represents the scientifically accepted duration of the YD event (Haug et al., 2001; Johnsen et al., 1997). Note that the x-scales top and bottom have been offset within the combined chronological uncertainty of the NGRIP and WE stalagmite records.

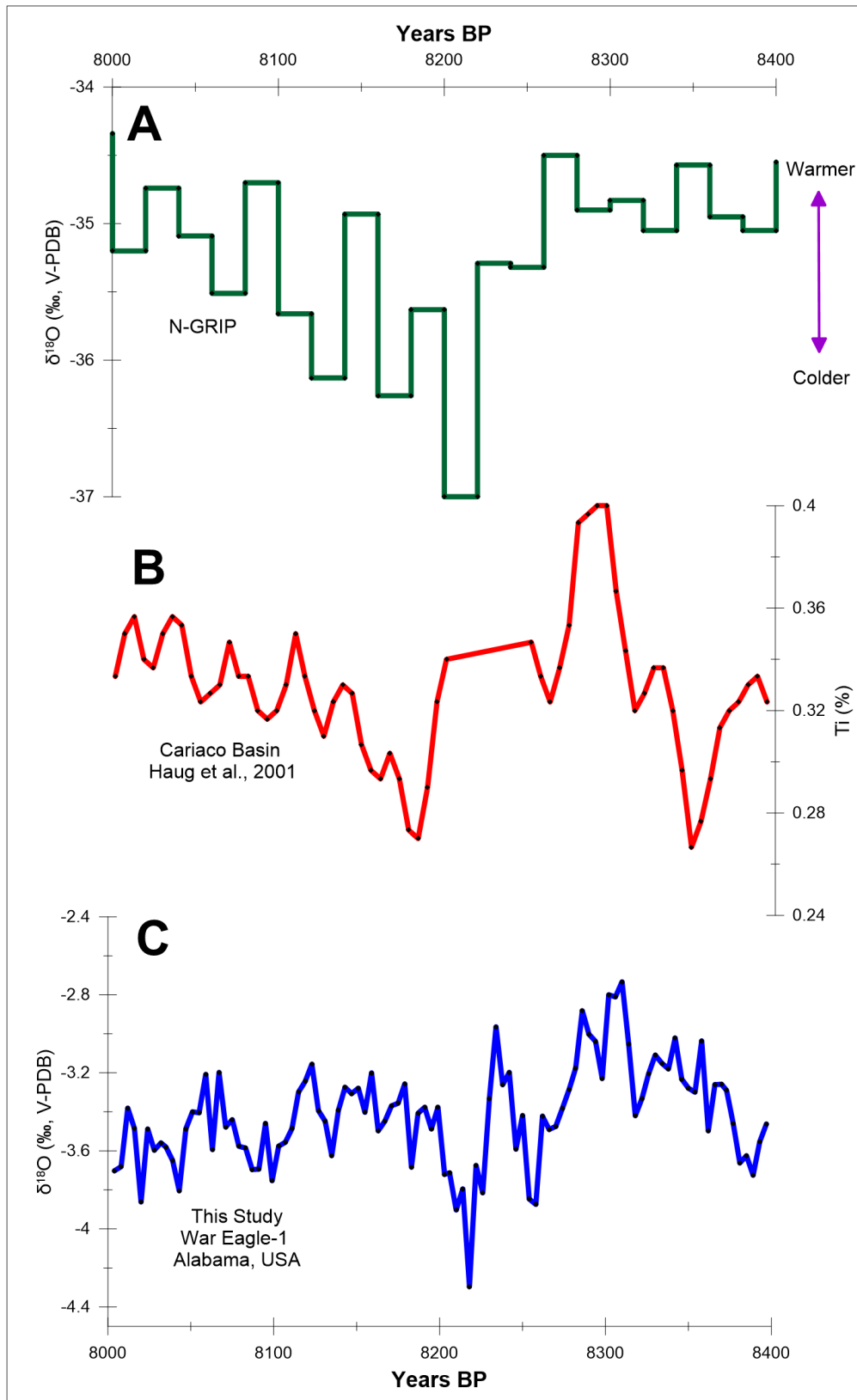


Figure 7: Comparison between WE-1 $\delta^{18}\text{O}$ record (C), the Cariaco Basin Ti% record (B), and NGRIP (A) (Haug et al., 2001; Johnsen et al., 1997).

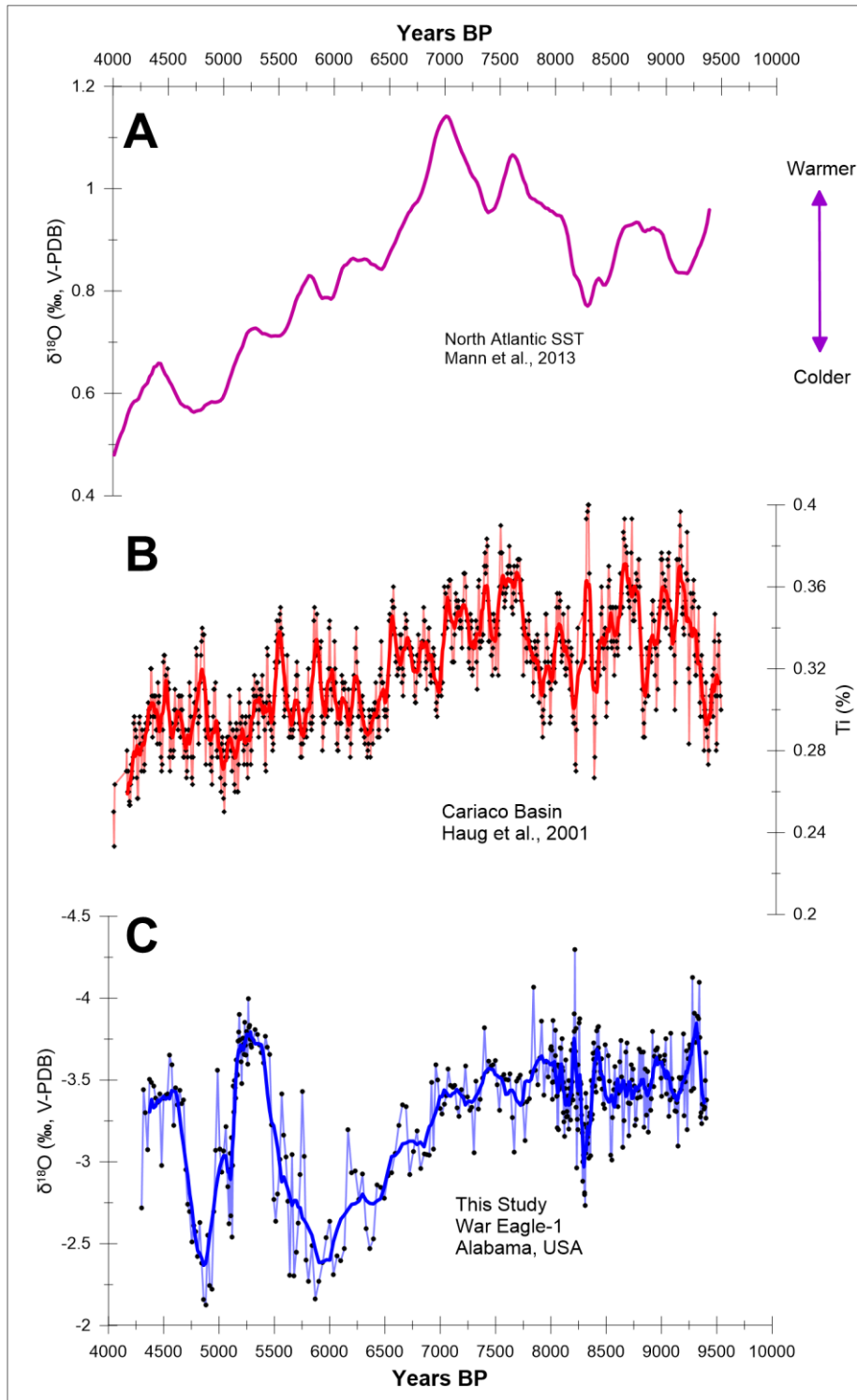


Figure 8: Comparison between WE-1 mid-Holocene $\delta^{18}\text{O}$ record (C), Cariaco Basin Ti% record (B), and North Atlantic sea surface temperatures (A). WE-1 possesses a darker blue line, which represents a running average to smooth out variability and a lighter blue line that is the $\delta^{18}\text{O}$ record. Plot B also has the same running average superimposed over the Ti% record (Haug et al., 2001; Mann et al., 2013).

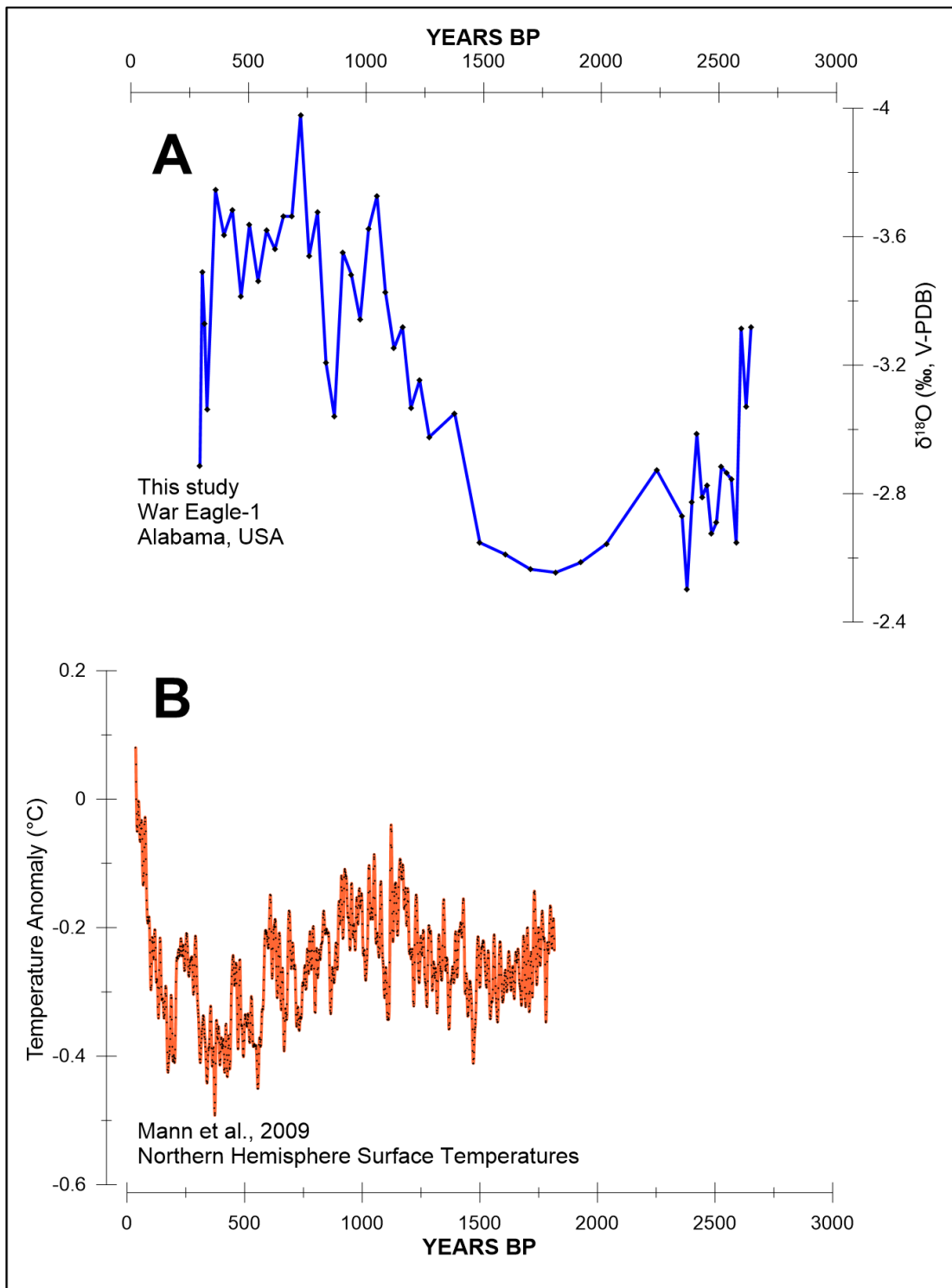


Figure 9: A Comparison between WE-1 $\delta^{18}\text{O}$ record (A) and northern surface temperatures (B) (Mann et al., 2009).

a. Climate Interpretation of WE stalagmite $\delta^{18}\text{O}$ record

The amount effect is well documented within tropical to subtropical regions (Dansgaard, 1964; Rozanski et al., 1993; Vuille et al., 2003) but has not been well documented within the interior SEUS, although some modeling data with isotope tracers suggest its potential existence in the southernmost extension of this region (Vuille et al., 2003). Relevant studies by Dhungana and Aharon (2019) and Lambert and Aharon (2010) have suggested that there is a weak amount effect on interannual timescales examining a couple of years, although their studies do not explicitly calculate the amount effect on interannual timescales typically observed on time scales of a decade or longer (Vuille et al., 2003).

Examination of precipitation amount (P) and precipitation $\delta^{18}\text{O}$ (δP) data (2005-2015), reveals an amount effect ($\delta P/\Delta P = -0.0017$ ‰ per mm) on interannual timescales ($r=0.34$) (Figure 3A). Removal of three anomalous years suggests a much stronger amount effect ($\delta P/\Delta P = -0.003$ ‰ per mm) ($r=0.92$) (Figure 3B). The available instrumental record remains too short to best characterize the amount effect on long time scales, highlighting the value of the effort by the University of Alabama to collect the only data available to date and the need to continue supporting this type of monitoring efforts, especially in order to understand the underlying driving mechanism of precipitation $\delta^{18}\text{O}$ variability, examine the role of regional and large-scale climate dynamical processes in controlling this variability, and help validate models with isotope tracers (Vuille, 2018; Vuille et al., 2003).

Correlation analyses between the amount of precipitation during the four climatological seasons and the seasonal amount-weighted $\delta^{18}\text{O}$ composition of rainfall from 2005-2015, suggest that winter precipitation amount variability has the least influence on interannual rainfall $\delta^{18}\text{O}$ variability (amount weighted) ($r=-0.07$), followed with increasing influence by spring ($r=-0.10$)

and fall seasons ($r=-0.16$) and the largest influence from summer precipitation ($r=-0.34$) (Figure 4). Notably, analysis of this data indicates that only during the summer there is a clear amount effect in Alabama on interannually (Figure 4). There is also a weaker amount effect on interannual timescales regarding the spring season and practically no evidence of an amount effect during the fall and winter seasons (Figure 4). Winter precipitation $\delta^{18}\text{O}$ varies the least interannually with average seasonal $\delta^{18}\text{O}$ compositions of $-5.3 \pm 0.9\text{‰}$ (1 SD). Summer precipitation $\delta^{18}\text{O}$ shows the most positive $\delta^{18}\text{O}$ average and the largest interannual amplitude variability ($-3.8 \pm 1.2\text{‰}$). We note that the most positive winter precipitation $\delta^{18}\text{O}$ value of -4.5‰ is significantly more negative and does not overlap with the most positive summer $\delta^{18}\text{O}$ values (-1.6‰ to -3.6‰ , $n=6$ years) whereas summer rainfall $\delta^{18}\text{O}$ can be as negative (-4.6‰ to -5.9‰ , $n=4$ years) as typical winter $\delta^{18}\text{O}$ values ($-5.3 \pm 0.9\text{‰}$). Finally, we highlight the potential negative isotopic influence of tropical cyclones, as exemplify by our direct analysis of Hurricane Michael rainfall (March 2019) with $\delta^{18}\text{O}$ composition of -11.2‰ . We finally, point out that the rainfall $\delta^{18}\text{O}$ composition determined in Auburn from October 2018 to March 2019 fall within values obtained for those months in the previous instrumental record from Tuscaloosa (Dhungana and Aharon, 2019). What drives the observed amount effect on interannual timescales?

As mentioned above, the lowest annual $\delta^{18}\text{O}$ values can be explained by typical winter precipitation contributions and by significant summer precipitation events. This implies that large precipitation events during the summer could be enough to explain the most negative annual isotopic composition of rainfall even when there was no rainfall associated with the other seasons, including winter. It also implies that negative annual rainfall $\delta^{18}\text{O}$ compositions, and of a stalagmite, do not *per se* reflect a stronger winter influence relative to summer. Nor that

observed rainfall annual positive isotopic values (and of a stalagmite) necessarily reflect dominance of summer precipitation relative to the other seasons. As an example, the instrumental record (2005-2015) indicates that the most positive annual $\delta^{18}\text{O}$ composition observed in the ten-year record were associated to low precipitation amounts during both summer and winter, while winter precipitation amount was still higher than summer.

The highest observed annual rainfall $\delta^{18}\text{O}$ values, on the other hand, can only be explained by lower spring and summer precipitation, the two seasons with the positive isotopic compositions capable of producing such values. The spring and summer rainfall positive $\delta^{18}\text{O}$ influence on annual rainfall $\delta^{18}\text{O}$, however, is contingent upon the amount effect on one hand and the relative contribution of the other seasons to the annual precipitation amount budget. Importantly, the dependence of this influence on the amount effect, implies that because the most positive $\delta^{18}\text{O}$ composition of summer and spring precipitation are associated with the lowest rainfall amounts (because of the amount effect), their influence on the annual isotopic budget decreases with precipitation amount. On the other hand, this influence is also contingent upon precipitation amount during the other seasons, fall and winter. Thus, the most positive annual rainfall $\delta^{18}\text{O}$ would be reached when spring and summer precipitation reach their minima, in conjunction with complete absence of fall and winter precipitation. This, of course, would imply a very different climate regime than observed today, and more closely resembling what is observed in the Caribbean and Gulf of Mexico regions today.

b. *Expected equilibrium stalagmite $\delta^{18}\text{O}$ values*

A necessary condition to interpret the oxygen isotopic composition of stalagmite calcite to reflect precipitation $\delta^{18}\text{O}$ variability is that calcite $\delta^{18}\text{O}$ is precipitated under isotopic equilibrium conditions. There is still not consensus on the exact equilibrium factor between

carbonates and water under specific environmental and drip water chemical conditions (Daëron et al., 2019). We apply a number of empirical and experimental “equilibrium” equations (Kim and O’Neil, 1997; Tremaine et al., 2011; Friedman and O’Neil, 1977; Chacko and Deines, 2008; Affek et al., 2014; Hansen et al., 2019) to approximate an expected stalagmite $\delta^{18}\text{O}$ composition based on the observed cave air temperature 14.7°C and range of annual amount-weighted $\delta^{18}\text{O}$ composition of rainfall over the 10-year instrumental record from Tuscaloosa, Alabama (i.e. -5.9‰ to -3.9‰). We note that because of the difficult accessibility to the cave we were only able to characterize the isotopic composition of drip water from at one drip site over the course of one year. As reported, cave drip water results agree with rainfall observations from previous years.

Equilibrium calculation results suggest that calcite precipitated at or near equilibrium conditions, assuming no surface evaporative water loss and that drips on timescales of a year or longer, accurately represent the same integration of rainfall $\delta^{18}\text{O}$, would produce calcite $\delta^{18}\text{O}$ compositions ranging from -6.6‰ , to -2.9‰ (Table 3). We note that the stalagmite $\delta^{18}\text{O}$ record will not necessarily only reflect the rainfall isotopic range observed today based on the relatively short instrumental record available (i.e. a decade long). On the other hand, stalagmite $\delta^{18}\text{O}$ variability is expected to reflect persisting multiyear shifts in the isotopic composition of rainfall because of the stalagmite sampling resolution (7-44 years). The WE isotopic results, however, fall within the calculated range using these multiple empirical equations (Table 3). We note that because WE does not have distinctive annual or shorter term laminations we were not able to produce a Hendy Test (Hendy, 1971). This test, however, is in most cases difficult to conduct as required in order to be diagnostically meaningful even when laminations are visible (Dorale and Liu, 2009). The observed different isotopic amplitude variability between the WE stalagmite

$\delta^{18}\text{O}$ and $\delta^{13}\text{C}$, whereby the $\delta^{13}\text{C}$ time series is much smoother, over most of the record, also provides evidence that potential kinetic effects were minimal. This observation in conjunction the characteristics and physical conditions of WE cave (relative humidity $\sim 100\%$ and stable temperature), and isotopic equilibrium calculations (Table 2), suggest that WE's calcite was precipitated under or near isotopic equilibrium conditions and likely faithfully records precipitation $\delta^{18}\text{O}$ variability.

Considering the analysis presented, we interpret WE stalagmite $\delta^{18}\text{O}$ variability to reflect the precipitation amount effect observed on interannual timescales. We point out again, that this effect results from the typical fall-winter precipitation negative $\delta^{18}\text{O}$ composition in conjunction with the amount effect observed particularly during the summer season.

Table 3: Calcite equilibrium calculations suggest that calcite precipitated at or near equilibrium conditions would produce calcite $\delta^{18}\text{O}$ compositions ranging from -6.6 ‰, to -2.9 ‰. (Kim and O'Neil, 1997; Tremaine et al., 2011; Friedman and O'Neil, 1977; Chacko and Deines, 2008; Affek et al., 2014; Hansen et al., 2019)

$\delta^{18}\text{O}$ dripwater	$\delta^{18}\text{O}$ water V-PDB	Temp (°C)	Mean Temp (°K)	$\delta^{18}\text{O}$ calcite modification of (Tremaine et al., 2011) based on (Kim et al., 2007)	$\delta^{18}\text{O}$ calcite (Tremaine et al., 2011)	$\delta^{18}\text{O}$ calcite (Friedman and O'Neil, 1977)	$\delta^{18}\text{O}$ calcite (Chacko and Deines, 2008)	$\delta^{18}\text{O}$ (Affek and Zaarur et al., 2014)	$\delta^{18}\text{O}$ (Affek and Zaarur et al., 2014)	$\delta^{18}\text{O}$ calcite (Hansen et al., 2019) A VG	$\delta^{18}\text{O}$ calcite (Hansen et al., 2019)	$\delta^{18}\text{O}$ calcite (Hansen et al., 2019)
-5.9	-35.42	14.7	287.9	-5.6	-6.6	-5.5	-5.9	-5.9	-5.1	-4.9	-4.9	-4.8
-3.9	-33.5	14.7	287.9	-3.7	-4.6	-3.5	-3.9	-3.9	-3.1	-2.9	-2.9	-2.9

c. Younger Dryas

Figure 6 places the WE stalagmite $\delta^{18}\text{O}$ -precipitation record in the context of high-latitude and Caribbean climate variability during the YD event. The pattern of hydroclimate variability suggested by the new stalagmite $\delta^{18}\text{O}$ record, suggests that the SEUS became progressively wetter during the YD. This pattern contrasts with that inferred for the Caribbean that suggests a decline in summer precipitation at the time, as implied by paleoclimate and global circulation model experiments. It is unlikely that summer precipitation increased in the SEUS during the YD because SSTs were lower in the main sources of moisture to this region (Gimeno et al., 2012; Li et al., 2013; Schmidt and Lynch-Stieglitz, 2011), the ITCZ was displaced south in summer (Paterson and Haug, 2006), and the size of the Atlantic warm pool was likely reduced, producing lower contributions of moisture to the Gulf of Mexico and the southeast US (Drumond et al., 2011). We note, on the other hand, that because there is no amount effect during the Winter season in the SEUS today, we cannot directly infer an increase in precipitation in winter from the negative shift in stalagmite as if a result of this effect. A stalagmite negative isotopic shift from the most positive values in the record while summer precipitation in the moisture source regions into the SEUS declined, would suggest that winter precipitation increased in absolute terms. This increase in winter precipitation was large enough to counteract the positive isotopic shift associated with lower summer precipitation dictated by the amount effect, which is strong during this season. We finally note that the observed negative stalagmite $\delta^{18}\text{O}$ shift during the YD could also reflect regional atmospheric cooling via the same-sign relationship between water condensation temperature and precipitation $\delta^{18}\text{O}$, although global circulation models suggest that precipitation $\delta^{18}\text{O}$ in the SEUS would not have change significantly (LeGrande et al., 2006). Lastly, a negative shift in precipitation $\delta^{18}\text{O}$ (and stalagmite) in the SEUS region is unlikely a reflection of negative isotopic pulses from the melting of the Laurentide ice sheet into the Gulf of Mexico region via the Mississippi River, because the observed stalagmite shifts are too late to be explained these pulses (Condrón and Winsor, 2012).

d. 8.2 ka Event

The WE stalagmite shows a significant negative $\delta^{18}\text{O}$ anomaly that coincides remarkably in duration and shape with the sharp isotopic shift observed in Greenland ice core records identified as the 8.2 ka event (Thomas et al., 2007) (Figure 7). This stalagmite isotopic anomaly is mimicked by the $\delta^{13}\text{C}$ record from the same archive, both showing a peak low at 8.25-8.2 kyr BP, suggesting a coeval hydrological shift with Greenland climate (Figure 5). Similarly, the 8.2 ka event in the stalagmite $\delta^{18}\text{O}$ record coincides temporally with an anomaly in the CB Ti% record, which shows a sharp peak low in Ti% between 8.25 and 8.15 kyr BP, reflecting aridity due to reduced northward migration of the ITCZ in summer (Figure 7b) (Peterson and Haug, 2006). In contrast, a single sharp anomaly at 8.25–8.1 kyr BP in the greyscale record reflects enhanced intensities of the trade winds, which affect this region in winter (Hughen et al., 1996) (not shown). Similar to what we argue for the YD event, we propose that the WE stalagmite negative $\delta^{18}\text{O}$ anomaly during the 8.2 ka event reflects a significant increase in winter precipitation, in line with the evidence of winter hydroclimate from the CB and precipitation increase in the SEUS suggested by global circulation models (LeGrande et al., 2006; Renssen et al., 2002).

e. Mid-Holocene Climate Variability

The MH section of the WE stalagmite shows a long-term positive isotopic shift coeval, within age uncertainties, with long-term cooling of the North Atlantic region generally attributed to a decrease in northern hemisphere summer insolation (Wanner et al., 2011) (Figure 8). The climate transition suggested by the stalagmite record occurs during the so-called Holocene Thermal Maximum (also called ‘Holocene Climate Optimum’, ‘Altithermal’ or ‘Hypsithermal’) in the Northern Hemisphere between about 7 and 4.2 ka BP. Northern Hemisphere cooling was associated with a progressive southern movement of the ITCZ, increasing summer drought in the Caribbean and a weakening of the Northern Hemisphere summer monsoon (Braconnot et al., 2007; Wanner et al., 2011)(Figure 8). This is a similar pattern observed during the rapid cooling events in the North Atlantic associated with the YD and 8.2 ka event but in contrast, the stalagmite $\delta^{18}\text{O}$ record suggests instead the SEUS became progressively drier,

probably reflecting a progressive decline in both winter and summer precipitation. Progressive increased aridity in the SEUS accompanies the transition from the ‘Holocene Climate Optimum’ to the ‘Neoglacial’, which was dominated by decreasing summer temperatures in the Northern Hemisphere driven by decreasing insolation during the boreal summer (Porter and Denton, 1967; Denton and Karlén, 1973). This drying trend suggested by the WE stalagmite was interrupted by two prominent isotopic reversals at 6-4.5 kyr BP. Climate reversal are also represented by the other stalagmite $\delta^{18}\text{O}$ record from Alabama that spans the interval between ~6-1 ka BP (Aharon and Dhungana, 2018) (Figure 10). There is no evidence of a similar abrupt change in Caribbean hydroclimate and North Atlantic SSTs (Figure 8). A high-resolution stalagmite $\delta^{18}\text{O}$ record from West-Central Florida, does not show a similar long-term negative shift either (Pollock et al., 2016). We therefore conclude in light of the available paleoclimate records covering this time interval, that the speleothem records from Alabama are probably recording a regional signal, perhaps associated with changes in the Gulf of Mexico region, which represents one of the main moisture sources of winter and summer precipitation in the SEUS. We note finally that these isotopic reversals observed in the speleothem $\delta^{18}\text{O}$ records, are also observed in the WE stalagmite $\delta^{13}\text{C}$ record, also suggesting a hydrological change at the time (Figure 5).

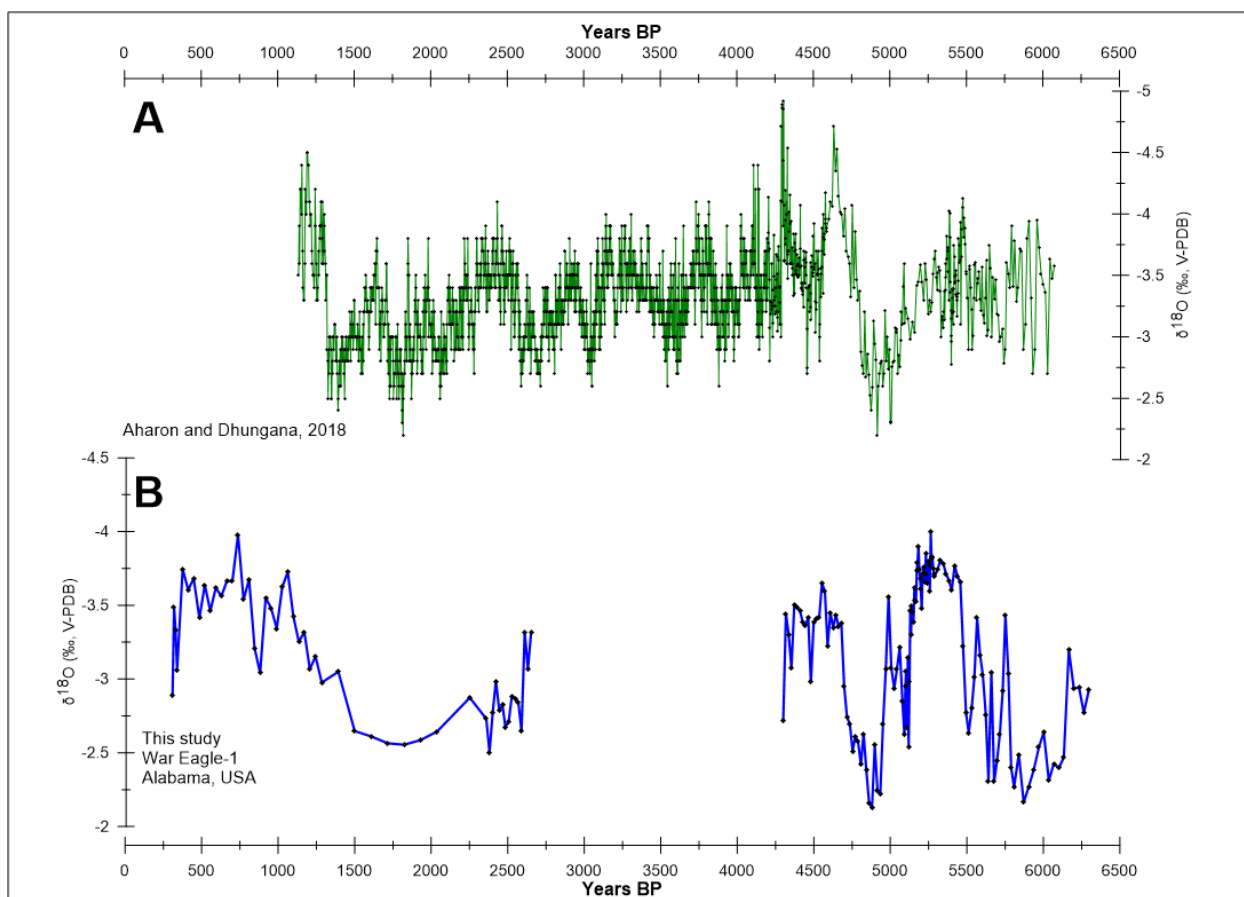


Figure 10 A Comparison between WE-1 $\delta^{18}\text{O}$ record (A) and a stalagmite record from Desoto Caverns, Alabama (B) (Aharon and Dhungana, 2018).

f. Late-Holocene Climate Variability

After a second hiatus, the WE stalagmite resumes growth at ~2.5 kyr BP and grew continuously until 0.3 kyr BP (Figure 9). Over this time the stalagmite $\delta^{18}\text{O}$ record shows a pattern similar to northern hemisphere and North Atlantic temperature variability whereby positive (negative) stalagmite isotopic values are associated with colder (warmer) Northern Hemisphere and North Atlantic temperatures (Mann et al., 2009). The stalagmite negative isotopic excursion coincides with the Little Ice Age interval, another period whereby the North Atlantic experienced cooling displacing the ITCZ southward and generating dry summer conditions in the Caribbean. Once again, SEUS winter precipitation increases as the North Atlantic cools and Caribbean precipitation declines in the summer. Tree ring chronologies from the

eastern SEUS spanning the last 1000 years do not suggest a similar shift in spring precipitation in the region (Stahle and Cleaveland, 1992). Tree ring records show large decadal variability but not a long-term shift as suggested by the WE stalagmite isotopic record, thus suggesting winter was the main driver of the stalagmite record.

g. Stalagmite Carbon Isotopes

Across the full length of the WE stalagmite, and during the prominent climate events highlighted above, the stalagmite $\delta^{13}C$ record mimics the oxygen isotope record. The carbon isotope response across these events could suggest hydrological shifts affecting vegetation type, density, and/or soil microbial productivity. Covariance between $\delta^{18}O$ and $\delta^{13}C$ can alternatively reflect shifts in karst hydrology whereby wetter conditions favor faster infiltration, decreased pCO_2 degassing and reduced prior calcite precipitation, ultimately producing lower $\delta^{13}C$ values (Fairchild and Treble, 2009). We note that the MH section of the stalagmite $\delta^{13}C$ record shifts from values typically associated with vegetation dominated by C4 plants to dominance of carbon with a bedrock origin (Fairchild and Baker, 2012). This offers complimentary evidence to the stalagmite $\delta^{18}O$ record of a decrease in annual precipitation particularly in summer season.

Conclusion

We produced the longest high-resolution stalagmite $\delta^{18}O$ record from Alabama and the Southeastern United States. We interpret this record to reflect an amount effect on interannual timescales and the relative contribution of summer relative to winter precipitation amount to the annual amount and isotopic budget. We find a close connection between hydroclimate variability in the SEUS, North Atlantic temperature variability and Caribbean hydroclimate. A consistent picture emerged whereby winter precipitation in the SEUS increases during events of high latitude cooling triggered by slowdown of North Atlantic deep-water formation, such as during the Younger Dryas and 8.2 ka cold events. In contrast, we find evidence suggesting that both summer and winter precipitation in the SEUS decrease across the transition from the ‘Holocene Climate Optimum’ to the ‘Neoglacial’, which is generally

attributed to external orbital forcing. Results from this study have implications to our understanding of hydroclimate responses in the southeastern United States resulting from the potential melting of the Greenland ice sheet and its influence on North Atlantic deep-water formation in a future dominated by an increasing greenhouse effect.

References

- Affek, H.P., Matthews, A., Ayalon, A., Bar-Matthews, M., Burstyn, Y., Zaarur, S., and Zilberman, T., 2014, Accounting for kinetic isotope effects in Soreq Cave (Israel) speleothems: *Geochimica et Cosmochimica Acta*, v. 143, p. 303–318, doi: 10.1016/j.gca.2014.08.008.
- Aharon, P., and Dhungana, R., 2017, Ocean-atmosphere interactions as drivers of mid-to-late Holocene rapid climate changes: Evidence from high-resolution stalagmite records at DeSoto Caverns, Southeast USA: *Quaternary Science Reviews*, v. 170, p. 69–81, doi: 10.1016/j.quascirev.2017.06.023.
- Alley, R.B., Mayewski, P.A., Sowers, T., Stuiver, M., Taylor, K.C., Clark, P.U., 1997. Holocene climate instability: a prominent widespread event 8200 yr ago. *Geology* 25, 483e486
- Alley, R.B., Ágústsdóttir, A.M., 2005. The 8k event: cause and consequences of a major Holocene abrupt climate change. *Quaternary Sci. Rev.* 24, 1123-1149.
- Anandhi, A., and Bentley, C., 2018, Predicted 21st century climate variability in southeastern U.S. using downscaled CMIP5 and meta-analysis: *Catena*, v. 170, p. 409–420, doi: 10.1016/j.catena.2018.06.005.
- Baigorria, G. A., Jones, J. W., and O'Brien, J. J., 2007, Understanding rainfall spatial variability in southeast USA at different timescales: *International Journal of Climatology*, v. 27, no. 6, p. 749-760.
- Barber, D.C., Dyke, A., Hillaire-Marcel, C., Jennings, A.E., Andrews, J.T., Kerwin, M.W., Bilodeau, G., McNeely, R., Southon, J., Morehead, M.D., Gagnon, J.-M., 1999. Forcing of the cold event of 8,200 years ago by catastrophic drainage of Laurentide lakes. *Nature* 400, 344-348.
- Barlow, M., 2011, Influence of hurricane-related activity on North American extreme precipitation: *Geophysical Research Letters*, v. 38, no. 4.

- Berger, W., 1990, The younger dryas cold spell—a quest for causes: *Palaeogeography, Palaeoclimatology, Palaeoecology*, v. 89, p. 219–237, doi: 10.1016/0031-0182(90)90063-d.
- Braconnot, P., Otto-Bliesner, B., Harrison, S., Joussaume, S., Peterchmitt, J. Y., Abe-Ouchi, A., Crucifix, M., Driesschaert, E., Fichefet, T., Hewitt, C. D., Kageyama, M., Kitoh, A., Lâiné, A., Loutre, M. F., Marti, O., Merkel, U., Ramstein, G., Valdes, P., Weber, S. L., Yu, Y., and Zhao, Y., 2007, Results of PMIP2 coupled simulations of the Mid-Holocene and Last Glacial Maximum – Part 1: experiments and large-scale features: *Clim. Past*, v. 3, no. 2, p. 261-277.
- Braconnot, P., Harrison, S., Kageyama, M., Bartlein, P., Masson-Delmotte, V., Abe-Ouchi, A., Otto-Bliesner, B., and Zhao, Y., 2012, Evaluation of climate models using palaeoclimatic data: *Nature Climate Change*, p. 417–424, doi: <https://doi.org/10.1038/nclimate1456>.
- Broecker, W. S., Kennett, J. P., Flower, B. P., Teller, J. T., Trumbore, S., Bonani, G., and Wolfli, W., 1989, Routing of meltwater from the Laurentide Ice Sheet during the Younger Dryas cold episode: *Nature*, v. 341, no. 6240, p. 318-321.
- Chacko, T., and Deines, P., 2008, Theoretical calculation of oxygen isotope fractionation factors in carbonate systems: *Geochimica et Cosmochimica Acta*, v. 72, p. 3642–3660, doi: 10.1016/j.gca.2008.06.001.
- Cheng, H., Edwards, R.L., Shen, C.-C., Polyak, V.J., Asmerom, Y., Woodhead, J., Hellstrom, J., Wang, Y., Kong, X., Spötl, C., Wang, X., and Alexander, E.C., 2013, Improvements in ²³⁰Th dating, ²³⁰Th and ²³⁴U half-life values, and U–Th isotopic measurements by multi-collector inductively coupled plasma mass spectrometry: *Earth and Planetary Science Letters*, v. 371-372, p. 82–91, doi: 10.1016/j.epsl.2013.04.006.

- Clark, P. U., S. J. Marshall, G. K. C. Clarke, S. W. Hostetler, J. M. Licciardi, and J. T. Teller (2001), Freshwater forcing of abrupt climate change during the last glaciation, *Science*, 293, 283–287, doi:10.1126/science.1062517.
- Climate Data Online - National Oceanic and Atmospheric ..., <https://www7.ncdc.noaa.gov/CDO/country> (accessed April 2020).
- Condron, A., and Winsor, P., 2012, Meltwater routing and the Younger Dryas: Proceedings of the National Academy of Sciences, v. 109, no. 49, p. 19928-19933.
- Cronin, T.M., 2010, *Paleoclimates: understanding climate change past and present*: New York, Columbia University Press.
- Curtis, S., 2008, The Atlantic multidecadal oscillation and extreme daily precipitation over the US and Mexico during the hurricane season: *Climate Dynamics*, v. 30, no. 4, p. 343-351.
- Daëron, M., Drysdale, R. N., Peral, M., Huyghe, D., Blamart, D., Coplen, T. B., Lartaud, F., and Zanchetta, G., 2019, Most Earth-surface calcites precipitate out of isotopic equilibrium: *Nature Communications*, v. 10, no. 1, p. 429.
- Dahl, K. A., Broccoli, A. J., and Stouffer, R. J., 2005, Assessing the role of North Atlantic freshwater forcing in millennial scale climate variability: a tropical Atlantic perspective: *Climate Dynamics*, v. 24, no. 4, p. 325-346.
- Dansgaard, W., 1964, Stable Isotopes in Precipitation: *Tellus*, v. 16, no. 4, p. 436-468.
- Denton, G.H., and Karlén, W., 1973, Holocene Climatic Variations—Their Pattern and Possible Cause: *Quaternary Research*, v. 3, p. 155–205, doi: 10.1016/0033-5894(73)90040-9.
- Deplazes, G., Lückge, A., Peterson L. C., Timmermann, A., Hamann, Y., Hughen K. A., Röhl, U., Laj, C., Cane, M. A., Sigman, D. M., and Haug, G. H., 2013, Links between tropical rainfall and North Atlantic climate during the last glacial period: *Nature Geoscience*, v. 6, p. 213-217.

- Dhungana, R., and Aharon, P., 2019, Stable isotopes and trace elements of drip waters at DeSoto Caverns during rainfall-contrasting years: *Chemical Geology*, v. 504, p. 96–104, doi: 10.1016/j.chemgeo.2018.11.002.
- Dominguez, F., Kumar, P., Liang, X.-Z., and Ting, M., 2006, Impact of Atmospheric Moisture Storage on Precipitation Recycling: *Journal of Climate*, v. 19, no. 8, p. 1513-1530.
- Done, J., Hu, A. X., Farmer, E. C., Yin, J. J., Bates, S., Frappier, A. B., Halkides, D. J., Kilbourne, K. H., Sriver, R., and Woodruff, J., 2009, The Thermohaline Circulation and Tropical Cyclones in Past, Present, and Future Climates: *Bulletin of the American Meteorological Society*, v. 90, no. 7, p. 1015-1017.
- Dorale, J. A., and Liu, Z. H., 2009, Limitations of Hendy Test Criteria in Judging the Paleoclimatic Suitability of Speleothems and the Need for Replication: *Journal of Cave and Karst Studies*, v. 71, no. 1, p. 73-80.
- Driese, S.G., Li, Z.-H., Cheng, H., Harvill, J.L., and Sims, J., 2007, 16. High-resolution rainfall records for middle and late Holocene based on speleothem annual UV fluorescent layers integrated with stable isotopes and U/Th dating, Raccoon Mountain Cave, Tennessee, USA: *Caves and Karst Across Time Geological Society of America Special Papers*, p. 231–246, doi: 10.1130/2016.2516(18).
- Drumond, A., Nieto, R., and Gimeno, L., 2011, On the contribution of the Tropical Western Hemisphere Warm Pool source of moisture to the Northern Hemisphere precipitation through a Lagrangian approach: *Journal of Geophysical Research: Atmospheres*, v. 116, no. D21.
- Enfield, D. B., 1996, Relationships of inter-american rainfall to tropical Atlantic and Pacific SST variability: *Geophysical Research Letters*, v. 23, no. 23, p. 3305-3308.

- Ellison, C.R.W., 2006, Surface and Deep Ocean Interactions During the Cold Climate Event 8200 Years Ago: *Science*, v. 312, p. 1929–1932, doi: 10.1126/science.1127213.
- Fairchild, I., and Treble, P., 2009, Trace elements in speleothems as recorders of environmental change: *Quaternary Science Reviews*, v. 28, p. 449-468.
- Fairchild, J., and Baker, A., 2012, *Speleothem Science: from Process to Past Environments*, Oxford, Wiley-Blackwell.
- Frappier, A. B., 2009, A stepwise screening system to select storm-sensitive stalagmites: Taking a targeted approach to speleothem sampling methodology (vol 187, pg 25, 2008): *Quaternary International*, v. 200, p. 120-121.
- Friedman, I., and Oneil, J., 1977, Compilation of stable isotope fractionation factors of geochemical interest: Professional Paper, doi: 10.3133/pp440kk.
- Gimeno, L., Stohl, A., Trigo, R. M., Dominguez, F., Yoshimura, K., Yu, L., Drumond, A., Durán-Quesada, A. M., and Nieto, R., 2012, Oceanic and terrestrial sources of continental precipitation: *Reviews of Geophysics*, v. 50, no. 4.
- Grimm, E.C., Watts, W.A., Jacobson, G.L., Hansen, B.C., Almquist, H.R., and Dieffenbacher-Krall, A.C., 2006, Evidence for warm wet Heinrich events in Florida: *Quaternary Science Reviews*, v. 25, p. 2197–2211, doi: <https://doi.org/10.1016/j.quascirev.2006.04.008>.
- Hansen, Jogvan; Jerram, Dougal; Ottley, Christopher; Widdowson, Mike (2019), “Hansen et al., 2019. Results of mixing calculations, fractionation calculations and partial melting calculations in association with a petrological study of selected basaltic rocks of the Faroe Islands.”, Mendeley Data, v1 <http://dx.doi.org/10.17632/47fzntf2b3.1>

- Haug, G. H., Hughen, K. A., Sigman, D. M., Peterson, L. C., and Röhl, U., 2001, Southward Migration of the Intertropical Convergence Zone Through the Holocene: *Science*, v. 293, no. 5533, p. 1304-1308.
- Hendy, C. H., 1971, The isotopic geochemistry of speleothems—I. The calculation of the effects of different modes of formation on the isotopic composition of speleothems and their applicability as palaeoclimatic indicators: *Geochimica Et Cosmochimica Acta*, v. 35, no. 8, p. 801-824.
- Hughen, K. A., Overpeck, J. T., Peterson, L. C., and Trumbore, S., 1996, Rapid climate changes in the tropical Atlantic region during the last deglaciation: *Nature*, v. 380, no. 6569, p. 51-54.
- Jakobsson, M., Løvlie, R., Arnold, E., Backman, J., Polyak, L., Knutsen, J.-O., and Musatov, E., 2001, Pleistocene stratigraphy and paleoenvironmental variation from Lomonosov Ridge sediments, central Arctic Ocean: *Global and Planetary Change*, v. 31, p. 1–22, doi: 10.1016/s0921-8181(01)00110-2.
- Johnsen, S.J., Clausen, H.B., Dansgaard, W., Gundestrup, N.S., Hammer, C.U., Andersen, U., Andersen, K.K., Hvidberg, C.S., Dahl-Jensen, D., Steffensen, J.P., Shoji, H., White, J., Jouzel, J., Fische, D., 1997. The d18O record along the Greenland Ice Core Project deep ice core and the problem of possible Eemian climatic instability. *J. Geophys. Res.* 102, 26,397e26,410
- Karmalkar, A. V., Bradley, R. S., and Diaz, H. F., 2011, Climate change in Central America and México: regional climate model validation and climate change projections: *Climate Dynamics*, v. 37, p. 605-629.
- Keim, B., 1996, Spatial, Synoptic, and Seasonal Patterns of Heavy Rainfall in the Southeastern United States: *Physical Geography*, v. 17, p. 313-328.

- Kim, S.-T., and Oneil, J.R., 1997, Equilibrium and nonequilibrium oxygen isotope effects in synthetic carbonates: *Geochimica et Cosmochimica Acta*, v. 61, p. 3461–3475, doi: 10.1016/s0016-7037(97)00169-5.
- Konrad, C. E., 1997, Synoptic-Scale Features Associated with Warm Season Heavy Rainfall over the Interior Southeastern United States: *Weather and Forecasting*, v. 12, no. 3, p. 557-571.
- Konrad II, C. E., and Perry, L. B., 2010, Relationships between tropical cyclones and heavy rainfall in the Carolina region of the USA: *International Journal of Climatology*, v. 30, no. 4, p. 522-534.
- Lambert, W.J., and Aharon, P., 2010, Oxygen and hydrogen isotopes of rainfall and dripwater at DeSoto Caverns (Alabama, USA): Key to understanding past variability of moisture transport from the Gulf of Mexico: *Geochimica et Cosmochimica Acta*, v. 74, p. 846–861, doi: 10.1016/j.gca.2009.10.043.
- Lases-Hernandez, F., Medina-Elizalde, M., Burns, S., and Decesare, M., 2019, Long-term monitoring of drip water and groundwater stable isotopic variability in the Yucatán Peninsula: Implications for recharge and speleothem rainfall reconstruction: *Geochimica et Cosmochimica Acta*, v. 246, p. 41–59, doi: 10.1016/j.gca.2018.11.028.
- Lea, D. W., Pak, D. K., Peterson, L. C., and Hughen, K. A., 2003, Synchronicity of Tropical and High-Latitude Atlantic Temperatures over the Last Glacial Termination: *Science*, v. 301, no. 5638, p. 1361-1364.
- LeGrande, A. N., Schmidt, G. A., Shindell, D. T., Field, C. V., Miller, R. L., Koch, D. M., Faluvegi, G., and Hoffmann, G., 2006, Consistent simulations of multiple proxy responses to an abrupt climate change event: *Proceedings of the National Academy of Sciences of the United States of America*, v. 103, no. 4, p. 837-842.

- Li, L., Li, W., and Barros, A. P., 2013, Atmospheric moisture budget and its regulation of the summer precipitation variability over the Southeastern United States: *Climate Dynamics*, v. 41, no. 3, p. 613-631.
- Liu, Z., Carlson, A. E., He, F., Brady, E. C., Otto-Bliesner, B. L., Briegleb, B. P., Wehrenberg, M., Clark, P. U., Wu, S., Cheng, J., Zhang, J., Noone, D., and Zhu, J., 2012, Younger Dryas cooling and the Greenland climate response to CO₂: *Proceedings of the National Academy of Sciences*, v. 109, no. 28, p. 11101-11104.
- Lohmann, G., and Lorenz, S., 2000, On the hydrological cycle under paleoclimatic conditions as derived from AGCM simulations: *Journal of Geophysical Research: Atmospheres*, v. 105, no. D13, p. 17417-17436.
- Magaña, V., Amador, A. J., and Medina, S., 1999, The Midsummer Drought over Mexico and Central America: *Journal of Climate*, v. 12, p. 1577-1588.
- Mann, M.E., Zhang, Z., Rutherford, S., Bradley, R.S., Hughes, M.K., Shindell, D., Ammann, C., Faluvegi, G., and Ni, F., 2009, Global Signatures and Dynamical Origins of the Little Ice Age and Medieval Climate Anomaly: *Science*, v. 326, p. 1256–1260, doi: 10.1126/science.1177303.
- Marcott, S.A., Shakun, J.D., Clark, P.U., and Mix, A.C., 2013, A Reconstruction of Regional and Global Temperature for the Past 11,300 Years: *Science*, v. 339, p. 1198–1201, doi: 10.1126/science.1228026.
- Matthes, F.E., 1939, Report of Committee on Glaciers, April 1939: *Transactions, American Geophysical Union*, v. 20, p. 518, doi: 10.1029/tr020i004p00518.
- Medina-Elizalde, M., Burns, S. J., Lea, D. W., Asmerom, Y., von Gunten, L., Polyak, V., Vuille, M., and Karmalkar, A., 2010, High resolution stalagmite climate record from the Yucatan

- Peninsula spanning the Maya terminal classic period: *Earth and Planetary Science Letters*, v. 298, no. 1-2, p. 255-262.
- Medina-Elizalde, M., Burns, S. J., Polanco-Martinez, J., Lases-Hernández, F., Bradley, R., Wang, H.-C., and Shen, C.-C., 2017, Synchronous precipitation reduction in the American Tropics associated with Heinrich 2: *Scientific Reports*, v. 7, no. 1, p. 11216.
- Medina-Elizalde, M., Polanco-Martinez, J. M., Lases-Hernandez, F., Bradley, R., and Burns, S., 2016, Testing the "tropical storm" hypothesis of Yucatan Peninsula climate variability during the Maya Terminal Classic Period: *Quaternary Research*, v. 86, no. 2, p. 111-119.
- Meltzer, D.J., and Holliday, V.T., 2010, Would North American Paleoindians have Noticed Younger Dryas Age Climate Changes?: *Journal of World Prehistory*, v. 23, p. 1–41, doi: 10.1007/s10963-009-9032-4.
- Mo, K. C., and Schemm, J. E., 2008, Relationships between ENSO and drought over the southeastern United States: *Geophysical Research Letters*, v. 35, no. 15.
- Morrill, C., and Jacobsen, R.M., 2005, How widespread were climate anomalies 8200 years ago?: *Geophysical Research Letters*, v. 32, doi: 10.1029/2005gl023536.
- Nrcs USDA SOIL SURVEY: Web Soil Survey - Home, <https://websoilsurvey.sc.egov.usda.gov/App/HomePage.htm> (accessed April 2020).
- Oglesby, R., Maasch, K., and Saltzman, B., 1989, Glacial meltwater cooling of the Gulf of Mexico: GCM implications for Holocene and present-day climates: *Climate Dynamics*, v. 3, p. 115-133.
- Oster, J.L., Sharp, W.D., Covey, A.K., Gibson, J., Rogers, B., and Mix, H., 2017, Climate response to the 8.2 ka event in coastal California: *Scientific Reports*, v. 7, doi: 10.1038/s41598-017-04215-5.

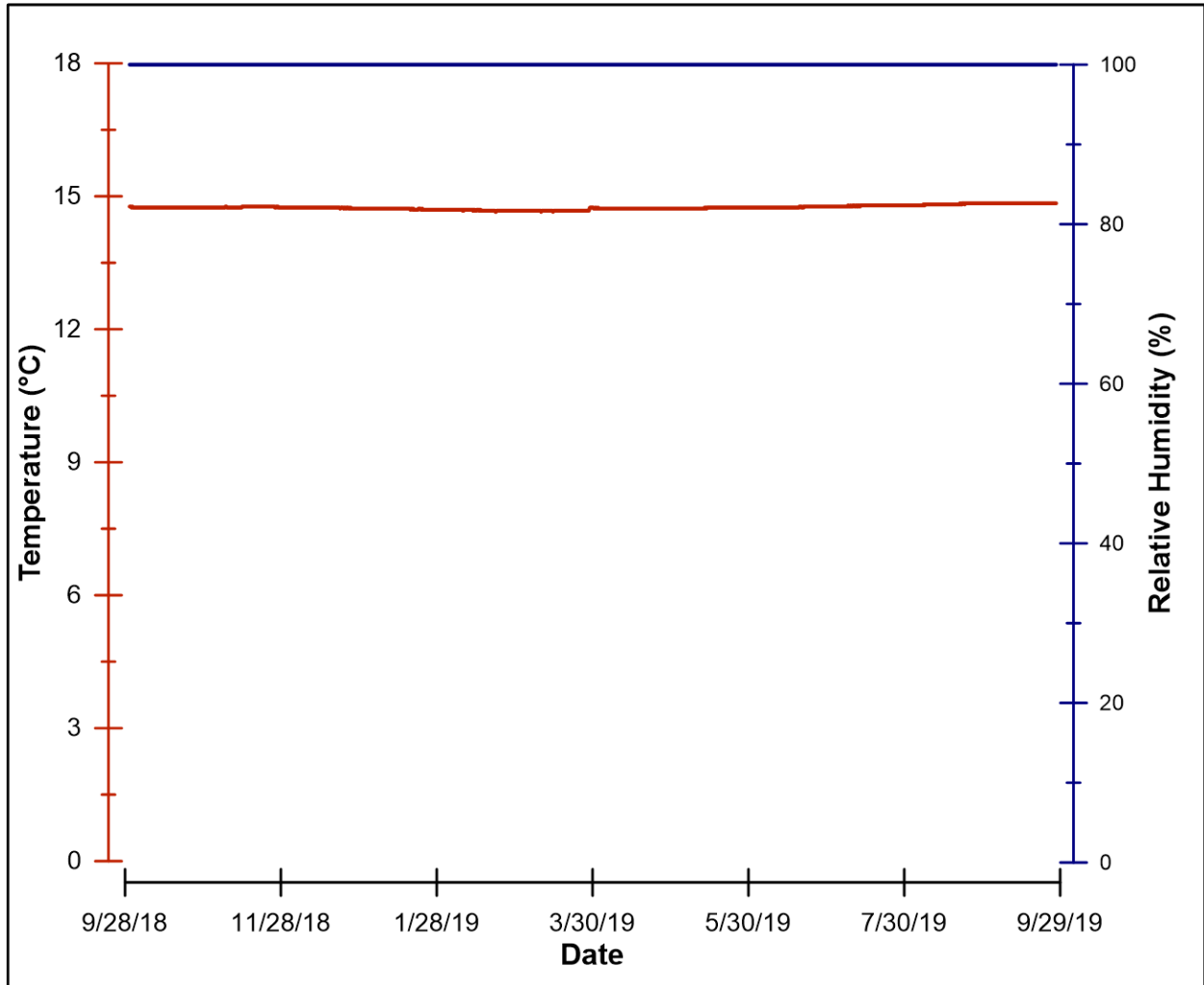
- Otto-Bliesner, B. L., and Brady, E. C., 2010, The sensitivity of the climate response to the magnitude and location of freshwater forcing: last glacial maximum experiments: *Quaternary Science Reviews*, v. 29, p. 56-73.
- Peterson, L. C., and Haug, G. H., 2006, Variability in the mean latitude of the Atlantic Intertropical Convergence Zone as recorded by riverine input of sediments to the Cariaco Basin (Venezuela): *Palaeogeography Palaeoclimatology Palaeoecology*, v. 234, no. 1, p. 97-113.
- Phipps, S.J., Mcgregor, H.V., Gergis, J., Gallant, A.J.E., Neukom, R., Stevenson, S., Ackerley, D., Brown, J.R., Fischer, M.J., and Ommen, T.D.V., 2013, Paleoclimate Data–Model Comparison and the Role of Climate Forcings over the Past 1500 Years: *Journal of Climate*, v. 26, p. 6915–6936, doi: 10.1175/jcli-d-12-00108.1.
- Pollock, A. L., van Beynen, P. E., DeLong, K. L., Polyak, V., and Asmerom, Y., 2016, A speleothem-based mid-Holocene precipitation reconstruction for West-Central Florida: *The Holocene*, v. 27, no. 7, p. 987-996.
- Porter, S.C., and Denton, G.H., 1967, Chronology of neoglaciation in the North American Cordillera: *American Journal of Science*, v. 265, p. 177–210, doi: 10.2475/ajs.265.3.177.
- Renssen, H., Goosse, H., and Fichefet, T., 2002, Modeling the effect of freshwater pulses on the early Holocene climate: The influence of high-frequency climate variability: *Paleoceanography*, v. 17, no. 2, p. 10-11-10-16.
- Renssen, H., Goosse, H., Roche, D.M., and Seppä, H., 2018, The global hydroclimate response during the Younger Dryas event: *Quaternary Science Reviews*, v. 193, p. 84–97, doi:10.1016/j.quascirev.2018.05.033.
- Rohling, E.J., Pälike, H., 2005. Centennial-scale climate cooling with a sudden cold event around 8200 years ago. *Nature* 434, 975-979.

- Rozanski, K., Araguás-Araguás, L., and Gonfiantini, R., Isotopic patterns in modern global precipitation in *Proceedings Climate Change in Continental Isotopic Records*, American Geophysical Union, 1993, Volume 78, Geophysical Monograph
- Schmidt, M. W., and Lynch-Stieglitz, J., 2011, Florida Straits deglacial temperature and salinity change: Implications for tropical hydrologic cycle variability during the Younger Dryas: *Paleoceanography*, v. 26, no. 4.
- Shen, C.-C., Edwards, R.L., Cheng, H., Dorale, J.A., Thomas, R.B., Moran, S.B., Weinstein, S.E., and Edmonds, H.N., 2002, Uranium and thorium isotopic and concentration measurements by magnetic sector inductively coupled plasma mass spectrometry: *Chemical Geology*, v. 185, p. 165–178, doi: [https://doi.org/10.1016/S0009-2541\(01\)00404-1](https://doi.org/10.1016/S0009-2541(01)00404-1).
- Shen, C.-C., Wu, C.-C., Cheng, H., Edwards, R.L., Hsieh, Y.-T., Gallet, S., Chang, C.-C., Li, T.-Y., Lam, D.D., Kano, A., Hori, M., and Spötl, C., 2012, High-precision and high-resolution carbonate ^{230}Th dating by MC-ICP-MS with SEM protocols: *Geochimica et Cosmochimica Acta*, v. 99, p. 71–86, doi: [10.1016/j.gca.2012.09.018](https://doi.org/10.1016/j.gca.2012.09.018).
- Shuman, B., 2002, The anatomy of a climatic oscillation: vegetation change in eastern North America during the Younger Dryas chronozone: *Quaternary Science Reviews*, v. 21, p. 1777–1791, doi: [10.1016/s0277-3791\(02\)00030-6](https://doi.org/10.1016/s0277-3791(02)00030-6).
- Stouffer, R. J., Yin, J., Gregory, J. M., Dixon, K. W., Spelman, M. J., Hurlin, W., Weaver, A. J., Eby, M., Flato, G. M., Hasumi, H., Hu, A., Jungclaus, J. H., Kamenkovich, I. V., Levermann, A., Montoya, M., Murakami, S., Nawrath, S., Oka, A., Peltier, W. R., Robitaille, D. Y., Sokolov, A., Vettoretti, G., and Weber, S. L., 2006, Investigating the Causes of the Response of the Thermohaline Circulation to Past and Future Climate Changes: *Journal of Climate*, v. 19, no. 8, p. 1365-1387.

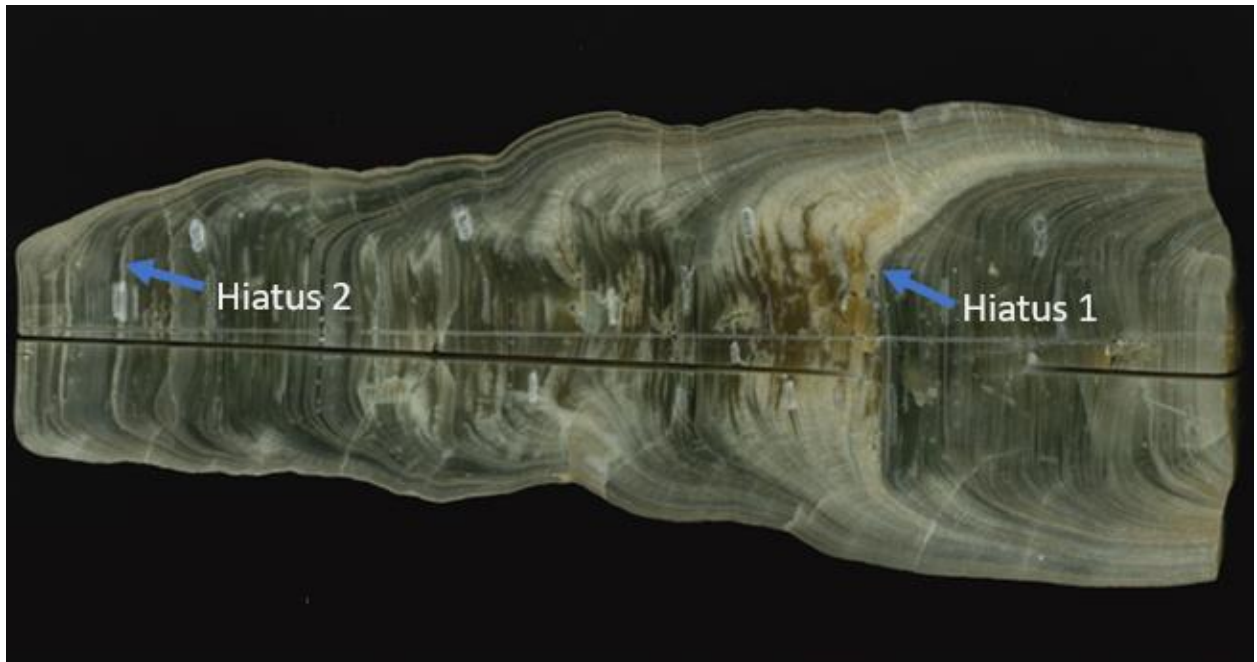
- Szabo, M.W., and Wheat, D.H., 1988, Geologic map of Alabama: Geological Survey of Alabama.
- Thomas, E.R., Wolff, E.W., Mulvaney, R., Steffensen, J.P., Johnsen, S.J., Arrowsmith, C., White, J.W., Vaughn, B., and Popp, T., 2007, The 8.2 ka event from Greenland ice cores: *Quaternary Science Reviews*, v. 26, p. 70–81, doi: <https://doi.org/10.1016/j.quascirev.2006.07.017>.
- Tremaine, D.M., Froelich, P.N., and Wang, Y., 2011, Speleothem calcite farmed in situ: Modern calibration of $\delta^{18}\text{O}$ and $\delta^{13}\text{C}$ paleoclimate proxies in a continuously-monitored natural cave system: *Geochimica et Cosmochimica Acta*, v. 75, p. 4929–4950, doi: [10.1016/j.gca.2011.06.005](https://doi.org/10.1016/j.gca.2011.06.005).
- Vellinga, M., and Wood, R. A., 2002, Global Climatic Impacts of a Collapse of the Atlantic Thermohaline Circulation: *Climatic Change*, v. 54, no. 3, p. 251-267.
- Vuille, M., 2018, Current state and future challenges in stable isotope applications of the tropical hydrologic cycle (Invited Commentary): *Hydrological Processes*, v. 32, no. 9, p. 1313-1317.
- Vuille, M., Bradley, R. S., Healy, R., Werner, M., Hardy, D. R., Thompson, L. G., and Keimig, F., 2003, Modeling delta O-18 in precipitation over the tropical Americas: 2. Simulation of the stable isotope signal in Andean ice cores: *Journal of Geophysical Research-Atmospheres*, v. 108, no. D6.
- Walsh, K. J. E., McBride, J. L., Klotzbach, P. J., Balachandran, S., Camargo, S. J., Holland, G., Knutson, T. R., Kossin, J. P., Lee, T. C., Sobel, A., and Sugi, M., 2016, Tropical cyclones and climate change: *Wiley Interdisciplinary Reviews-Climate Change*, v. 7, no. 1, p. 65-89.
- Wang, C., Lee, S.-K., and Enfield, D. B., 2008, Climate Response to Anomalously Large and Small Atlantic Warm Pools during the Summer: *Journal of Climate*, v. 21, no. 11, p. 2437-2450.

- Wang, H., Fu, R., Kumar, A., and Li, W., 2010, Intensification of Summer Rainfall Variability in the Southeastern United States during Recent Decades: *Journal of Hydrometeorology*, v. 11, no. 4, p. 1007-1018.
- Wanner, H., Solomina, O., Grosjean, M., Ritz, S. P., and Jetel, M., 2011, Structure and origin of Holocene cold events: *Quaternary Science Reviews*, v. 30, no. 21, p. 3109-3123.
- Wanner, H., Beer, J., Butikofer, J., and Widmann, M., 2008, Mid-to Late Holocene climate change: An overview: *Quaternary Science Reviews*, p. 1797–1828, doi: 10.1016/j.quascirev.2008.06.013.
- Yu, Z., and Wright, H., 2001, Response of interior North America to abrupt climate oscillations in the North Atlantic region during the last deglaciation: *Earth-Science Reviews*, v. 52, p. 333–369, doi: 10.1016/s0012-8252(00)00032-5.

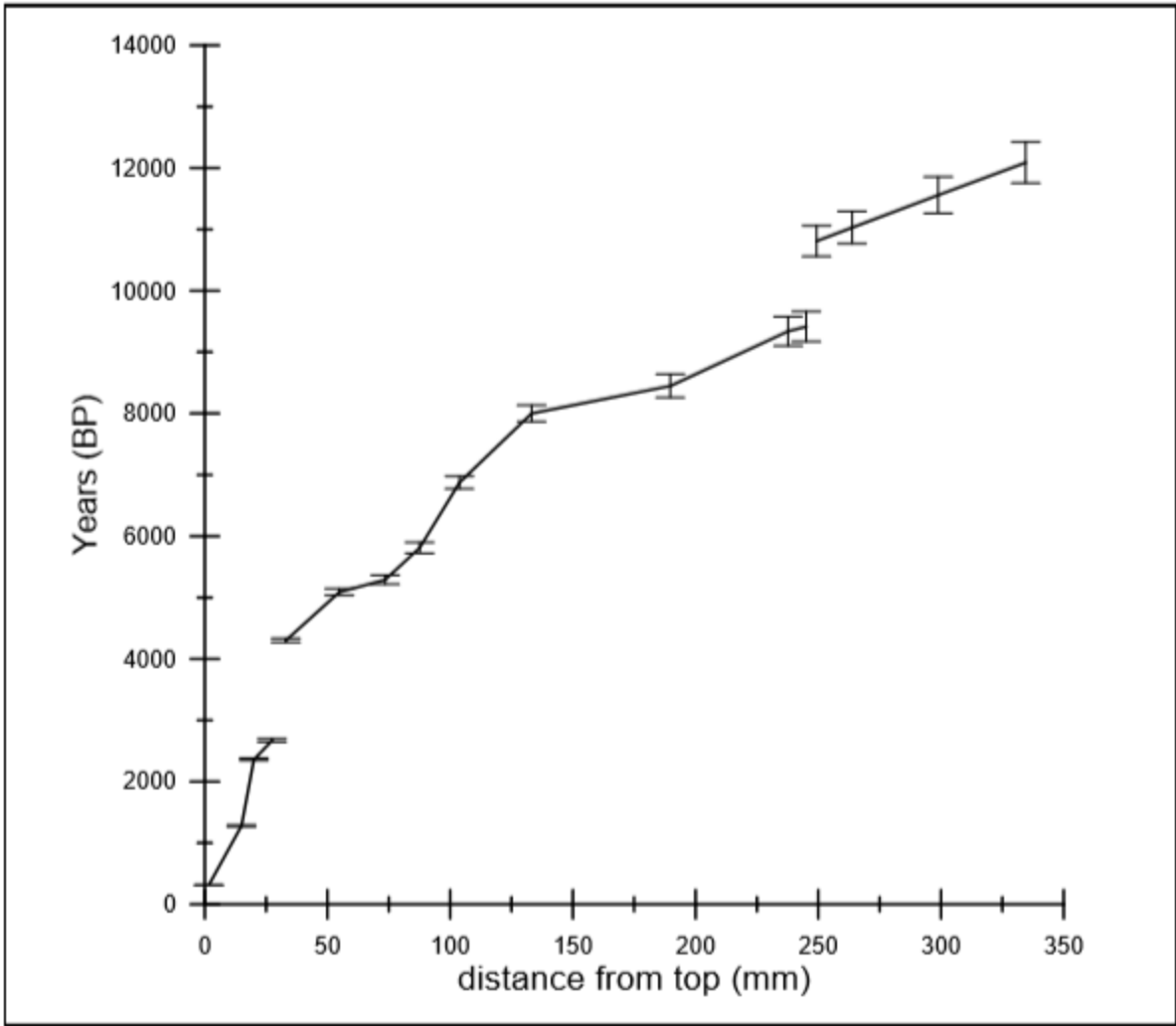
Supplementary Figures



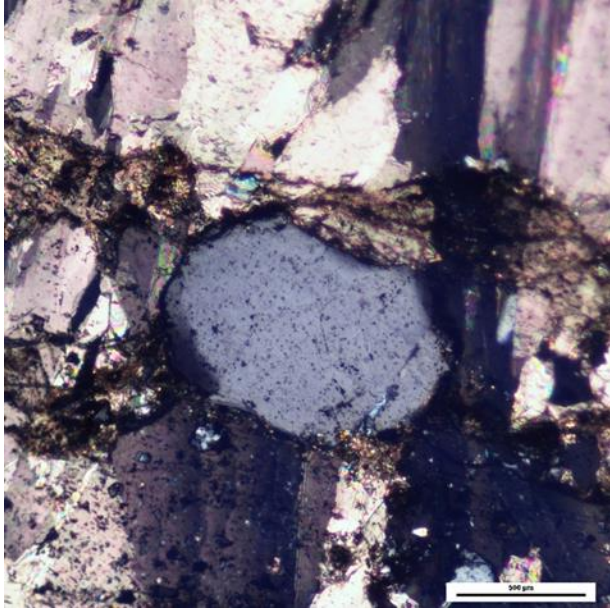
Supplementary Figure 1: Climate data record from ONSET HOBO software from September 2018 to September 2019. Relative Humidity stayed a constant 100% and the cave temperature remained constant year around at 14.7°C.



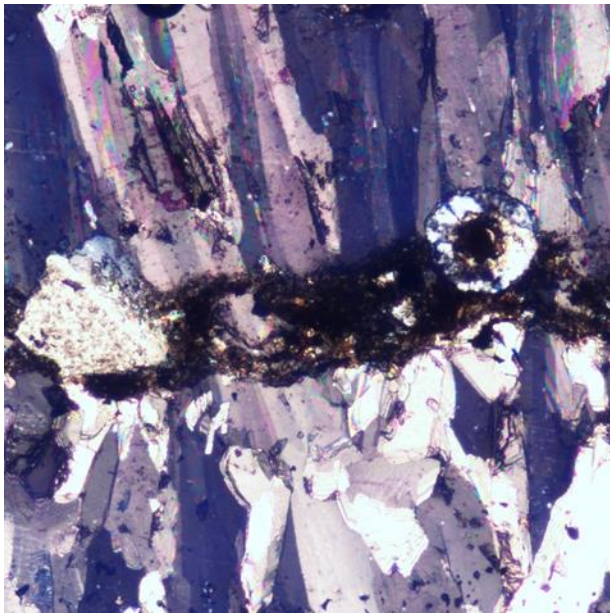
Supplementary Figure 2: Scan of War Eagle-1.



Supplementary Figure 3: War Eagle-1's mean age model was created by running a simple piecewise linear regression model.



Supplementary Figure 4: XPL photograph of Hiatus 1. A tectosilicate appears between two distinct boundaries within the hiatus.



Supplementary Figure 5: XPL photograph of hiatus 2. A possible sponge spicule is embedded within the apparent hiatus.